

Polymerization and replication of primordial RNA explained by clay-water interface dynamics

Carla Alejandre,^{1,2,*} Adrián Aguirre-Tamaral,^{3,4,*} Carlos Briones,³ and Jacobo Aguirre^{1,2,†}

¹Centro de Astrobiología (CAB), CSIC-INTA), Carretera de Ajalvir km 4, 28850 Torrejón de Ardoz, Madrid, Spain

²Grupo Interdisciplinar de Sistemas Complejos (GISC), Madrid, Spain

³Centro de Astrobiología (CAB), CSIC-INTA), Carretera de Ajalvir km 4, 28850 Torrejón de Ardoz, Madrid, Spain

⁴Department of Biology, University of Graz, Universitätsplatz 2, 8010 Graz, Austria

Abstract: RNA is the only known biopolymer that combines genotype and phenotype in a single molecular entity. This has suggested that the flow of genetic information DNA-RNA-proteins already operating in LUCA could have been preceded by a primordial era when RNA was the genetic and catalytic macromolecule. However, understanding how RNA could have polymerized and subsequently replicated in early Earth remains challenging. We present a theoretical and computational framework to model the non-enzymatic polymerization of ribonucleotides and the template-dependent replication of primordial RNA molecules, at the interfaces between the aqueous solution and a clay mineral supplied by its interlayers and channels. Our results demonstrate that efficient polymerization and accurate replication of single-stranded RNA polymers, sufficiently long to fold and acquire basic functions (> 15 nt), were possible at clay-water interfaces in early Earth, provided the physico-chemical environment exhibited an oscillatory pattern of large amplitude and a period compatible with spring tide dynamics. Interestingly, the theoretical analysis presents rigorous evidence that RNA replication efficiency increases in oscillating environments compared to constant ones. Moreover, the versatility of our framework enables comparisons between different genetic alphabets, showing that a four-letter alphabet –particularly when allowing non-canonical base pairs, as in current RNA– represents an optimal balance of replication speed and sequence diversity in the pathway to life.

Significance statement: *RNA, a biopolymer capable of carrying genetic information and performing biochemical functions, is thought to have played a key role in the origin of life. However, how RNA initially formed and replicated in early Earth, around 4 Gyr ago, remains unknown. Our study presents a theoretical and computational framework showing that a clay-water interface in oscillating environmental conditions, such as those driven by spring tide dynamics, could have enabled efficient RNA polymerization and accurate template-dependent replication. This discovery highlights the potential influence of large moons on the emergence of life in planetary environments. In parallel, our results underscore the evolutionary advantage of RNA's four-letter genetic alphabet in generating diverse, functional sequences critical for the origin and early evolution of life.*

The origin of life on Earth is a fundamental question that remains elusive when we aim to fully describe it in physico-chemical terms. For a complex enough molecular system to be considered alive, it must exhibit and combine a number of features such as compartmentation, energy dissipation, replication of a genetic material and metabolism, thus allowing its self-reproduction and open-ended evolution. In the earlier stages of the pre-cellular world, simple mechanisms at the molecular level, still not catalyzed by enzymes, must have driven the increasing complexity of prebiotic molecules. Different sets of chemical species needed to be concentrated and separated from the external environment through some form of surface- or membrane-based compartmentalization. A small fraction of them could have been used as monomers to build (by means of non-enzymatic polymerization mechanisms) progressively longer and more complex polymeric molecules, some of which were endowed

with heritable information that provided a substrate for Darwinian evolution to act upon [1–4].

Since the pioneering work of Alexandr I. Oparin a century ago [5] and of John B.S. Haldane five years later [6], particularly over the past four decades, various hypotheses have emerged to try to understand the transition from chemistry to biology. One model that gained significant attention since the 1980s is the RNA World hypothesis [7–9]. According to its current version, in the framework of prebiotic systems chemistry, the first self-reproducing entities contained single-stranded RNA (ssRNA) as genetic material, as well as a proto-metabolism based on ribozymes: structured ssRNA molecules endowed with catalytic activities (including RNA ligase and RNA polymerase), likely assisted by short abiotic peptides and low molecular weight compounds as cofactors [1, 10, 11].

However, before the establishment of an RNA (or RNA-peptide) world, the available and, somehow, chemically activated ribonucleotides (from now on, termed nts) should have polymerized into ssRNA oligomers in absence of the catalytic activity of ribozymes. Additionally, a non-enzymatic process of template-dependent

*These two authors contributed equally

†jaguirre@cab.inta-csic.es

RNA replication could have ensured the availability of populations of RNA molecules with related sequences, on which selection could act [12]. Indeed, the minimum length of an RNA polymerase ribozyme (i.e., a structured RNA molecule capable of replicating other RNA molecules used as templates) has been estimated in the range of 165 nts [13] to 182 nts [14–16], which is far longer than the up to 50-mer ssRNA molecules that can be experimentally obtained by means of non-enzymatic polymerization using activated nts and montmorillonite clay as a catalyst [17–19]. Therefore, random RNA polymerization of short oligomers, which is known to be favored by clays and other heterogeneous media [20–23], could have been followed by a ligation-based, stepwise process of modular evolution of RNA that allowed the assembly of a template-dependent RNA polymerase ribozyme [24, 25]. Non-enzymatic, template-dependent RNA replication has been explored both experimentally [26–29] and through theoretical models, most of them focusing on liquid environments [30–40]. However, little work has focused on the entire process, connecting RNA polymerization and template-dependent replication in the same heterogeneous environment and from a global, systems chemistry perspective [1, 41, 42].

The vast diversity of geological environments that coexisted in early Earth opens up a multitude of possible chemical reactions and physical scenarios, not all equally conducive to the establishment of an RNA world. Under specific conditions, ssRNA polymers can grow in thermal environments subjected to extreme temperature changes [43, 44], while other models have explored RNA growth and ligation in temperate aqueous environments [34, 45] or in dry conditions [46]. Interestingly, extensive work suggests that oscillating environments were crucial for the emergence of life [47–52]. These fluctuating conditions were abundant in early Earth and could be of various types. For instance, while Lathe proposed two decades ago that tides at ocean shores could have provided the oscillating driving force for the origin of replicating biopolymers [53, 54], Fernando *et al.* noted that temperature, nt concentration and tidal oscillations considered in these works might provoke a biopolymer elongation that would hinder its accurate replication [33]. Anyway, temperature oscillations and wet/dry cycles have received the most attention: temperature cycles are known to promote the hybridization/denaturation of complementary ssRNA strands [55], while dehydration periods are essential to allow condensation reactions, such as the formation of 3'-5' phosphodiester bonds necessary for RNA polymerization [49, 56].

Numerous studies have experimentally demonstrated that the surfaces of certain minerals and rocks, in particular clays such as montmorillonite, exhibit chemical and crystallographical properties (including their microscopic structure, distribution of cations and spacing of the phyllosilicate interlayers) that can favor the adsorption and correct orientation of nts while providing a locally anhydrous environment, thus catalyzing the abiotic

polymerization of RNA [17–21, 50, 57–59]. The importance of including clay surfaces in the prebiotic context is further highlighted by studies showing that the behavior of RNA polymers differs significantly between aqueous environments and aqueous-clay interfaces [60]. In particular, the sedimentation of ssRNA oligomers on clay surfaces or other minerals induces a phase separation into oligonucleotide-dense and dilute phases that can facilitate the selection of specific RNA sequences with prebiotic functions [61].

Despite the aforementioned research conducted on the comparison among potential physico-chemical contexts for the origin of life, we are still far from unveiling the precise mechanisms that led to the emergence and replication of the first RNA polymers, around 4 Gyr ago [3, 62, 63]. To shed light on this subject, we propose an integrative numerical and theoretical approach that considers both non-enzymatic RNA polymerization and template-dependent replication in an environment where nts and ssRNA polymers interact through a clay-water interface. We introduce EarlyWorld, a computational framework supported by a theoretical model, which allows us to test how different environmental conditions could affect the polymerization and replication of ssRNA oligomers. By exploring and refining our understanding of the specific fluctuating environments that could effectively promote the increase in biochemical complexity, we aim to identify the early Earth environments most suitable for the emergence of RNA populations, as a prerequisite for the origin of life.

I. METHODS: DESCRIPTION AND RULES OF THE MODEL

We have developed a computational environment called EarlyWorld to simulate the non-enzymatic RNA polymerization and template replication in primordial heterogeneous media, such as on the interface between an aqueous solution and a clay surface, in the absence of RNA polymerase ribozymes. Clays are known to present a complex structure of internal channels and interlayers, where water can get in and promote an intricate set of clay-water interfaces of around 100 m² per g of clay [64]. The RNA polymerization and replication processes computationally simulated here take place in two compartments of the clay showing different geochemical properties. Fig. 1 schematizes the dynamics described by EarlyWorld: Fig. 1A and B sketch the natural compartments of the model, and Fig. 1C and D show example realizations of the evolution with time of the system in each compartment. A rigorous explanation of the algorithm is provided in SI Appendix, Supporting Information Text S1, and information on the public availability of the code is found in SI Appendix, Supporting Information Text S2.

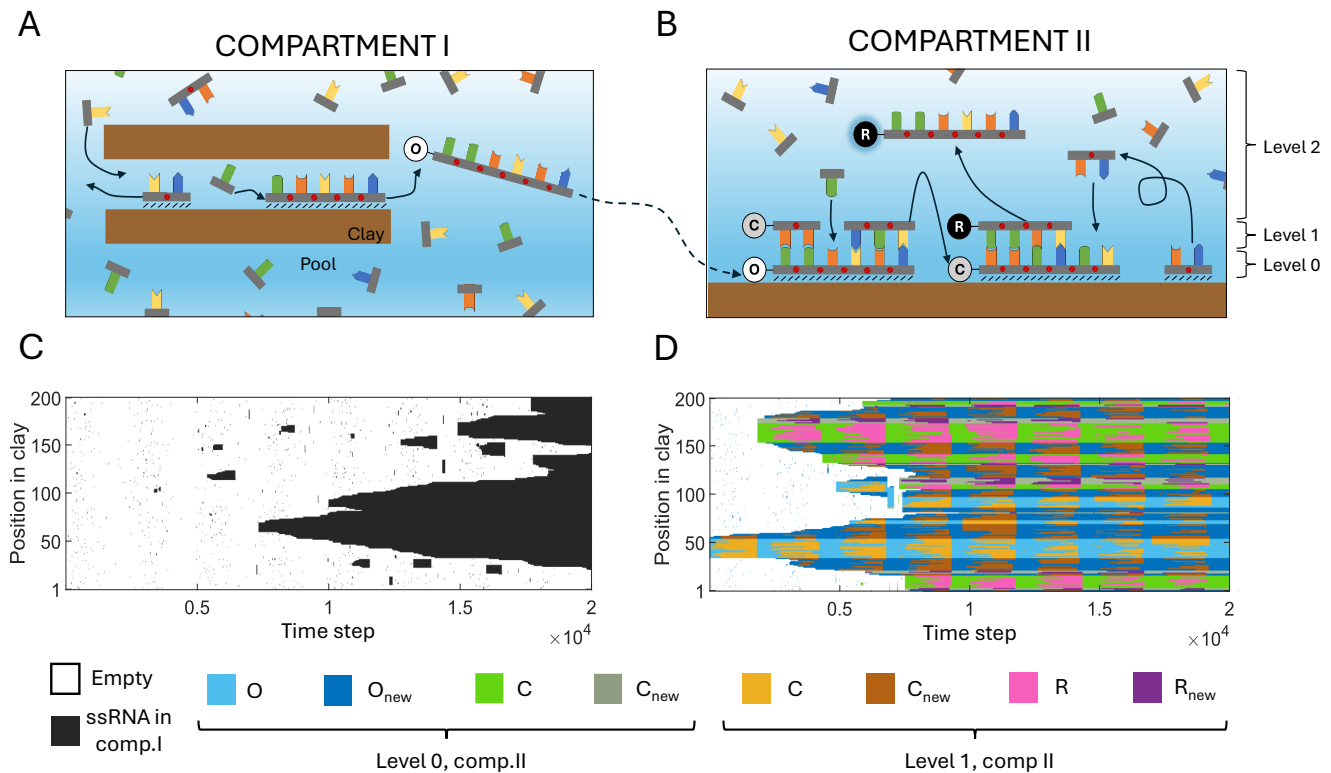


FIG. 1: Description of the non-enzymatic RNA polymerization and replication in an early Earth’s clay-water interface modeled by EarlyWorld. Top panels (A and B) sketch each natural compartment of the model and bottom panels (C and D) show example realizations of the evolution with time t of all the positions available in an oscillating clay environment. The bottom legend corresponds to the colors shown in panels C and D. If not said otherwise, throughout this work we will use clays of length $L = 200$ positions, $N = 1600$ nts equally distributed between A, G, C, U types and initially placed in the aqueous phase, $C \equiv G$ and $A = U$ nucleobase complementarities, and simulation times $t_{max} = 2 \times 10^4$ time steps. Compartment I: Random polymerization occurs due to the catalytic action of clays in an interlayer of a clay grain, where complementary base pairing is not permitted. Only clay-nt interactions (of strength α) are permitted and ssRNA can be formed at the clay surface. Compartment II: The template replication of the original strand O occurs involving complementary base pairing; strand C (complementary to O) is formed, denatured from the template, released to the pool and adsorbed to the clay. In a next step, the replication of strand C yields strand R, whose sequence is equal to the original ($R = O$). Once the dsRNA molecule C-R is formed, its denaturation will release the ssRNA oligomer R, completing the RNA replication process. Other polymers O_{new} spuriously formed in comp.II can also be used as template (C_{new}) and replicated (R_{new}). In comp.II both clay-nt (of strength α) and nt-nt (of strength β) interactions are allowed, and ssRNA molecules can remain adsorbed to the clay (level 0), hybridize to their complementary strand to form dsRNA (level 1), or move to the aqueous phase (level 2). In this example, $\alpha = 0.8 + 0.5 \sin(2\pi t/2500)$ and $\beta = 6 + 5.9 \sin(2\pi t/2500)$.

A. Compartment I

Random polymerization of nts takes place in compartment I (comp.I from now on) due to the catalytic action of clays. It represents an internal channel or interlayer that is wide enough to allow ssRNA, but not double-stranded (ds) RNA oligomers to pass through. This assumption is supported by experimental data showing that the A-helix of dsRNA has a diameter of ~ 2.4 nm [65], while the interlayer space for montmorillonite and other clays typically varies between 1.3 and 1.8 nm, depending on their ionic composition and hydration state [66]. In consequence, complementary base pairing is not possible here (Fig. 1A). The compartment has two differ-

ent levels: the clay-water interface (shortened to “clay”), and the aqueous phase (or “pool”). For simplicity, the clay level is described by a 1D-vector of length L where each element/position can be either empty or contain a single nt, while the aqueous phase is a *disordered box* with space for an unlimited number of nts and ssRNA molecules.

The clay and the pool will be enriched with ssRNA oligomers throughout each simulation, but every numerical realization in comp.I starts with the clay level totally empty and a number N of nts equally distributed between those composing the genetic alphabet in use (EarlyWorld accepts any genetic alphabet and base pairs of all kind, see section Results IIC). At each time step, one of the molecules in the pool is chosen randomly and

gets adsorbed to the clay in a randomly chosen place (involving one or more contiguous positions), as far as it is empty. Otherwise the molecule returns to the pool. In the clay, it will form a covalent (3'-5' phosphodiester) bond with other nts potentially placed at any (or both) of its adjacent positions. The resulting polymer remains attached to the clay, and we assume that its covalent sugar-phosphate backbone is unbreakable (as hydrolysis is not considered in this model). After that, every oligomer adsorbed to the clay can be released to the pool with a desorption probability of

$$P_\alpha = e^{-l\alpha}, \quad (1)$$

where the interaction parameter $\alpha > 0$ describes the strength of clay-nt interactions (due to Van der Waals forces and ionic bonds) in the environment that surrounds them, and l is the length (i.e., number of nts) of the polymer whose desorption is evaluated. Finally, note that only the oligomers detached from the clay into the pool are recorded as effectively produced in the process, because exclusively free and mobile ssRNA molecules can migrate to compartment II and continue the process.

B. Compartment II

Here, the compartment represents a wide internal channel, an inter-particle site or an external clay surface, and, in consequence, is able to accommodate both ssRNA and dsRNA molecules and template-dependent RNA replication based on complementary base pairing. Simulations start with the same number of nts of each type available in the pool and with an initial ssRNA molecule (original strand O from now on), consisting of 20 randomly chosen nts adsorbed to the clay in a random place. This ssRNA O represents a strand that is assumed to be formerly polymerized in comp.I, was released from it, eventually entered compartment II (comp.II from now on) and attached to the clay surface. Three levels are relevant for the evolution of the system: the clay or “level 0”, where nts and polymers can be adsorbed (as in comp.I); the complementary level or “level 1”, where one nt can only be placed if it is complementary to other nt included in a ssRNA oligomer which is placed in level 0 and thus contribute to the formation of dsRNA via hydrogen bonding; and the aqueous phase, pool or “level 2”, where free nts, ssRNA and dsRNA stay in solution. In each time step, a randomly chosen molecule in the pool interacts with a randomly chosen place in the surface of the clay. ssRNA and dsRNA of any length can be adsorbed to the clay in level 0, and ssRNA will be hybridized to other ssRNA strand adsorbed to the clay acting as a template in level 1 if they are fully complementary. After that, every ssRNA or dsRNA of length l in level 0 will have a desorption probability (i.e., probability of being released to the pool) of $P_\alpha = e^{-l\alpha}$, where α is the clay-nt interaction parameter already mentioned in comp.I. Also, every dsRNA (both attached to the clay

or free in the pool) can be denatured with a probability of

$$P_\beta = e^{-l\beta}, \quad (2)$$

where l stands for the dsRNA length, and the nt-nt interaction parameter $\beta > 0$ describes the strength of the hydrogen bond interactions established between their nucleobases in the environment that surrounds them.

Throughout each simulation, in comp.II the dynamics described will eventually release complementary C strands of the original O sequence to the pool (level 2), as well as complementary C_{new} strands of other newly-generated O_{new} sequences randomly polymerized in the clay (level 0). Interestingly, when a polymer C falls in an empty place of the clay and is adsorbed, it might become the template for a further polymerization based on nucleobase complementarity, and the denaturation of the dsRNA formed will release to the pool a ssRNA that is “complementary of the complementary C”: the strand replicate or R, equal (partially, or in its full length) to the original polymer O.

Our model describes the influence of the environment in the polymerization and replication of short ssRNA polymers through two parameters, α and β , which represent the global strength of clay-nt and nt-nt interactions, respectively. Changing these parameters mimics varying external physico-chemical magnitudes such as temperature, pH, ionic strength and presence of divalent cations, to cite a few. Large values of α and β represent mild environments that facilitate said interactions (and the concomitant formation of progressively longer ssRNA and dsRNA molecules), whereas low values represent harsh environments and have the opposite effect.

II. RESULTS

A. Compartment I: RNA polymerization on a clay surface

The polymerization process in comp.I depends exclusively on the clay-nt parameter α . Fig. 2 plots the length distribution of the ssRNA molecules (polymers from now on) that can be formed with the rules set of EarlyWorld for different environmental conditions, both constant and fluctuating. The length distribution of the polymers produced attached to the clay and desorbed back to the pool at any time step for different constant values of α reveals a steep decay in Fig. 2A, in full agreement with the assumed relationship between the abundance of polymerized ssRNA molecules and their length [38, 39, 67]. In this work we are specially interested in obtaining the potential largest polymer that can be produced in a given heterogeneous environment, as it could eventually be more structurally complex and functionally relevant than the shorter ones. Thus, Fig. 2B shows the distribution of the maximum polymer length obtained along every

realization for each parameter α (the detailed explanation of how maximum polymer lengths are obtained is provided in SI Appendix, Supporting Information Text S3). For $\alpha \rightarrow 0$ the environment is so harsh that every nt that reaches the clay is immediately desorbed from it and released back to the pool, while for $\alpha \rightarrow \infty$ the mild environment allows the adsorbed nts to polymerize fast and become strongly stuck to the clay surface. Both limits result in the presence of very short ssRNA oligomers in the pool. For intermediate α values, however, oligomers can be substantially polymerized but still be desorbed, reaching maximum polymer lengths of $\sim 5 - 12$ for $\alpha \sim 0.8$.

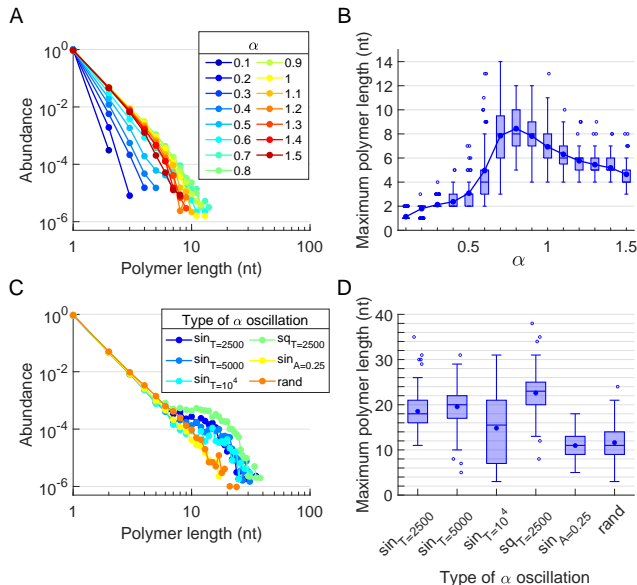


FIG. 2: Effect of constant and fluctuating environmental conditions on the polymerization of RNA catalyzed by a clay surface (comp.I). (A) Distribution of abundances of ssRNA k-mers (monomers, dimers, etc) and (B) maximum polymer length distributions over constant environments (clay-nt parameter α is constant with time). (C) Distribution of abundances of k-mers and (D) maximum polymer length distributions over six fluctuating environments (α varies with time): *sin* stands for sinusoidal oscillation, *sq* for square wave oscillation and *rand* for random fluctuation. If not said otherwise in the axes, $\alpha_0 = 0.8$, $A = 0.5$, $T = 2500$. Every simulation was repeated 100 times.

Fluctuating environments can be easily introduced in EarlyWorld by changing the value of the parameters α and β over time. Fig. 2C and D show, respectively, the length distribution of ssRNA molecules polymerized and desorbed from the clay, and the distribution of maximum polymer lengths obtained in every realization for several α -oscillating environments. Considering environmental oscillations of period T and amplitude A , the sinusoidal oscillatory environments studied follow $\alpha(t) = \alpha_0 + A \sin(2\pi t/T)$, square wave oscillations follow $\alpha(t) = \alpha_0 + A \operatorname{sgn}(\sin(2\pi t/T))$, and randomly fluctuating environments follow the continuous uniform distribution $\alpha(t) = U\{\alpha_0 - A, \alpha_0 + A\}$. The length distribution of

polymers plotted in Fig. 2C shows a power-law decay for the random environment that behaves as a lower limit for the rest of fluctuating environments, which, depending on their characteristics, show a larger or smaller hump for long (> 10 nt) polymer lengths. In Fig. 2D, it can be seen that, for all oscillating patterns, maximum polymer lengths notably increase with respect to those achieved in constant environments: means move from 1 – 9 nt for constant environments, with absolute maxima around 15 nt, to 10 – 24 nt for fluctuating ones, with absolute maxima around 40 nt.

B. Compartment II: Template-dependent RNA replication dynamics on a clay surface

The simplest secondary structures that ssRNA molecules can fold into are called stem-loops, consisting of a dsRNA stem closed by a terminal loop. In turn, hairpin structures are slightly more complex and contain a bulge within the stem, which can provide certain biochemical functionality to the molecule [68]. Thus, it is commonly assumed that ribozymes should contain at least 15 – 35 nts to be able to fold into complex enough structures [24]. As shown in the previous section, this polymer length interval can be typically obtained in EarlyWorld when the environment (parameter α) fluctuates. Accordingly, simulations in comp.II start with a 20 nt-long, random ssRNA polymer O adsorbed to the clay. Along each simulation, we record the complementary C and replicate R strands derived from the original O sequence, which are produced and released to the pool. Remarkably, Cs and Rs can contain, additionally to the accurate copy of the corresponding template, other random or spurious sequences attached to their 5' or 3' ends during the replication process, thus forming a longer molecule than the polymer O from which they derive [33]. For that reason, and in order to avoid the loss of identity of the RNA molecules that are being replicated, throughout this work we consider those C and R polymers that have an accuracy of $> 75\%$, i.e., their sequence is formed by $> 75\%$ of products of the original polymer O (see SI Appendix, Supporting Information Text S4 and Fig. S3 for detailed information on sequence accuracy and simulations with 100% accuracy, which yield equivalent results).

Both clay-nt parameter α and nt-nt parameter β play a role in the formation of C and R polymers in comp.II. Fig. 3 shows the effect of fluctuating environmental conditions (i.e., α and β) on the stepwise replication of the original 20 nt-long polymer O. Considering oscillations of period T_γ and amplitude A_γ , the sinusoidal oscillatory environments follow $\gamma(t) = \gamma_0 + A_\gamma \sin(2\pi t/T_\gamma)$, square wave oscillations follow $\gamma(t) = \gamma_0 + A_\gamma \operatorname{sgn}(\sin(2\pi t/T_\gamma))$, and randomly fluctuating environments follow the continuous uniform distribution $\gamma(t) = U\{\gamma_0 - A_\gamma, \gamma_0 + A_\gamma\}$, where $\gamma = \{\alpha, \beta\}$. When one parameter is constant and the other oscillates (Fig. 3A,B), β becomes the most lim-

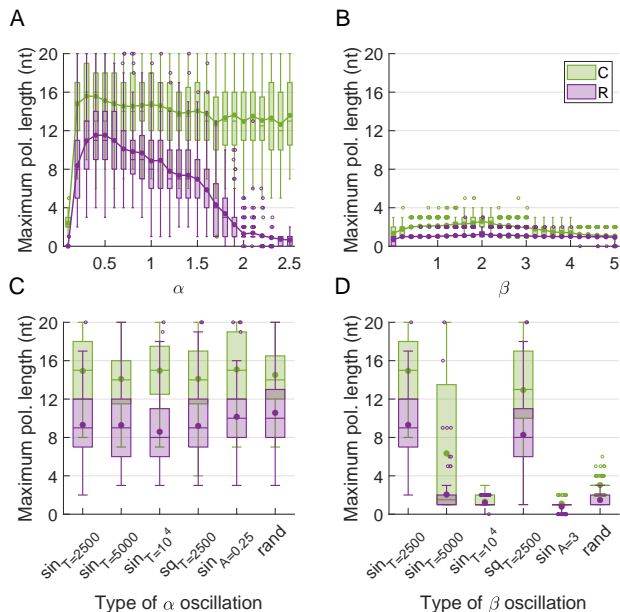


FIG. 3: Effect of environmental fluctuations on the template-dependent replication of a ssRNA molecule adsorbed to a clay surface (comp.II). (A) Maximum complementary (C, green in all panels) and replicate (R, purple in all panels) polymer length distributions for an oscillating β and a constant α parameter. (B) Maximum polymer length distributions for an oscillating α and a constant β parameter. (C) Maximum polymer length distributions for different α fluctuating patterns, with a fixed β oscillation. (D) Maximum polymer length distributions for different β fluctuating patterns, with a fixed α oscillation. Fluctuating environments: *sin* stands for sinusoidal oscillation, *sq* for pulse wave, *rand* for random fluctuation. If not said otherwise, $\alpha_0 = 0.8$, $A_\alpha = 0.5$, $T_\alpha = 2500$ and $\beta_0 = 6$, $A_\beta = 5.9$, $T_\beta = 2500$. Every simulation started with a random 20 nt-long ssRNA molecule, and was repeated 100 times.

iting factor. If β remains constant over time, only insignificant fractions of the original sequence O are replicated as R polymers. In contrast, a wide range of constant α values is compatible with the production of long C and R ssRNA molecules and allows the replication of the entire initial molecule O (Fig. 3A). Remarkably, long C polymers populate the pool but replication disappears for large constant α . The reason is that, in order to form Rs, there must be empty positions in the clay level where Cs can be adsorbed and serve as templates to produce Rs, but large α enhances the occupancy of positions in clay by monomers or short polymers, thus impairing the formation of Rs from Cs.

Fig. 3C and D show how simultaneous (but not necessarily similar) fluctuations in both α and β parameters affect the formation and length of C and R polymers. Results in Fig. 3C indicate that, for the different cases studied, maintaining a standard sinusoidal β oscillation while varying the period and amplitude of sinusoidal α oscilla-

tions (as well as changing it to a more abrupt pulse wave) does not significantly affect replication efficiency. The mean length of the obtained R polymers remains close to a 50% of the original O sequence, and the maximum value after 100 realizations of all oscillation patterns recovered the whole original sequence length (20 nts). On the contrary, maintaining an α oscillation compatible with high polymerization activity in comp.I and varying the period or amplitude of β oscillations drastically affects the system performance (Fig. 3D), presenting from a strong enhancement to a collapse of the replicative dynamics. In summary, EarlyWorld shows that efficient template replication of RNA is only plausible under oscillating environments, being their proficiency much more dependent on the properties of the nt-nt interactions that rule the template replication than on the clay-nt interplay that controls the initial RNA polymerization.

In Fig. 4, a more complete scan of the space of parameters for the template-dependent RNA replication that takes place in comp.II is presented. Without loss of generality, it is now assumed that (i) in natural environments the whole system formed of comp.I and II of a clay grain in contact with water will be exposed to the same oscillatory environmental conditions, thus affecting interaction parameters α and β with the same period $T_\alpha = T_\beta = T$, and (ii) the amplitude of such oscillations will be proportional to the average values α_0 and β_0 by a factor $f \in [0, 1]$ (i.e., $A_\alpha = f\alpha_0$ and $A_\beta = f\beta_0$). Fig. 4A shows the dependence of the replication efficiency on the average interaction parameters α_0 and β_0 and the amplitude fraction f (see Fig. S4 for the corresponding plots on the efficiency of the formation of the complementary strand C). As already observed in Fig. 3A, relatively low α_0 is optimal because, in order to form Rs, there must be free space in the clay for Cs to adsorb and serve as Rs' templates, a condition better satisfied with an environment that hampers the attachment to the clay. On the other side, large β_0 and very large amplitudes of the oscillations become necessary, as they represent environments that alternate periods of strong polymerization enhancement with periods of intense denaturation probability.

Fig. 4B shows the dependence of the replication efficiency on the α and β oscillation period. Short periods prevent from a sufficient elongation of the polymerized or replicated strands, the lower limit $T \rightarrow 0$ being comparable to a random distribution of β values (as shown in Fig. 3D). Intermediate period values favor the replicative dynamics, and copies of all lengths are densely represented. Remarkably, the value of the oscillation period that optimizes the replication dynamics ($T = 3000 \pm 500$ time steps) in Fig. 4B coincides with the number of simulation time steps that in average is required to form a complete 20-nt long complementary copy attached to the original O sequence ($\langle t_{20} \rangle \approx 3300$, see Fig. S5). This equivalence will be of the maximum importance to match simulation times with real time scales and allow EarlyWorld to generate testable predictions about prebiotic environments (see section Discussion). When oscillation

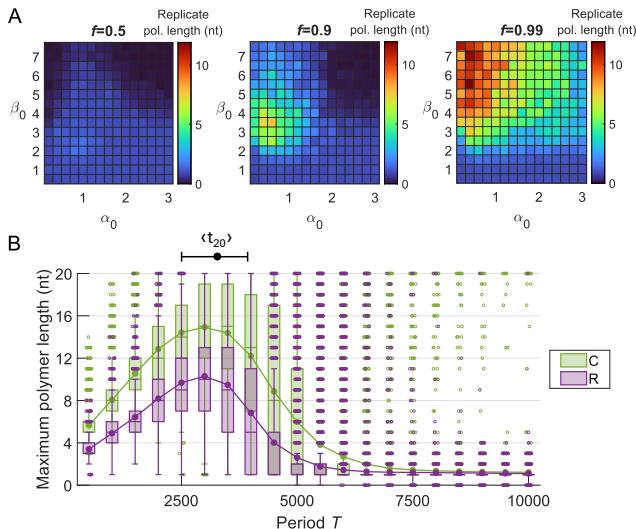


FIG. 4: Effect of the model parameters on the template-dependent replication of a ssRNA molecule adsorbed to a clay surface (comp.II). (A) Dependence of the mean of maximum R polymer lengths with average interaction parameters α_0 and β_0 at three different amplitude fractions f (being $A_\alpha = f\alpha_0$ and $A_\beta = f\beta_0$). $T_\alpha = T_\beta = 2500$. (B) Dependence of the maximum length distribution of C polymers (complementary, green) and R polymers (replicates, purple) on the oscillation period $T = T_\alpha = T_\beta$. $\alpha_0 = 0.8$, $A_\alpha = 0.5$ and $\beta_0 = 6$, $A_\beta = 5.9$. The mean time to polymerize a 20-nt long ssRNA by template-dependent polymerization ($\langle t_{20} \rangle$) is displayed with 25th-75th percentiles (see Fig. S5). Every simulation started with a random 20 nt-long ssRNA molecule, and was repeated 20 times in (A) and 10^4 times in (B).

periods become very large, a drastic transition occurs: the environment varies so slowly that the system resembles temporarily a β -constant environment (as shown in Fig. 3B), favoring an excessive polymerization of dsRNA molecules that do not denature in such conditions, leading to the concomitant collapse of the replication process. Interestingly, as it can be observed in Fig. S6, the maximum R polymer lengths observed for short periods follow log-normal distributions, become decreasing long-tailed distributions strongly peaked in 1 nt just after the transition, and finally collapse to the absence of any relevant replication for larger periods. Note the similarities with the first order transition between the regime dominated by self-sustaining populations of long sequences and that of free monomers thoroughly analyzed in [34]. Finally, let us remark that optimal periods, together with the value of α_0 used ($\alpha_0 = 0.8$), also optimized polymerization in comp.I (Fig. 2), strongly reinforcing the plausibility of observing in real systems the mechanism here presented for the polymerization and posterior replication of RNA molecules.

C. RNA replication across different genetic alphabets

The computational environment EarlyWorld can be used to test multiple physico-chemical conditions compatible with those present in the early Earth where RNA world was established. One of the most controversial questions about the origin and evolution of our genetic material deals with the number, relative concentration and pairing rules of different monomers that formed RNA (and, eventually, pre-RNA) polymers [1, 69, 70]. Current RNA is composed of four different nts, whose nucleobases interact specifically through hydrogen bonding: adenine and uracil (paired by means of two H bonds, $A=U$), as well as guanine and cytosine (linked by three H bonds, $G\equiv C$). In addition, non-canonical base pairs, such as Wobble base pairs (the most common type of these being $G=U$) are not infrequent in RNA, though they are less thermodynamically stable than canonical pairs. In order to shed light on why prebiotic chemistry chose one genetic alphabet among all possible ones, we used our computational model to test the polymerization and replication efficiency of six different options: two-letter alphabet [$A=U$] ($A2_{au}$), two-letter [$G\equiv C$] ($A2_{gc}$), canonical four-letter [$A=U, G\equiv C$] ($A4$), four-letter with additional Wobble base pair [$A=U, G\equiv C, G=U$] ($A4^*$, representing current RNA alphabet and pairing rules), and six-letter with a new base pair involving two unknown nucleotides (termed X and Y) linked by either two [$A=U, G\equiv C, X=Y$] ($A6_2$) or three hydrogen bonds [$A=U, G\equiv C, X\equiv Y$] ($A6_3$). The main properties of these alphabets when introduced in EarlyWorld are shown in Table I.

TABLE I: Parameters of the computational environment EarlyWorld and the theoretical model for different genetic alphabets, from 2 to 6 letters. s_A and t_A are normalizations (such that $s_A = t_A = 1$ for $A4$) of the average number of hydrogen bonds per nt and the connection time, respectively, used in the mathematical model.

Alphabet	H-bonds/nt	s_A	Connection time	t_A
$A2_{au}$	2	4/5	2	1/2
$A2_{gc}$	3	6/5	2	1/2
$A4$	5/2	1	4	1
$A4^*$	7/3	14/15	8/3	2/3
$A6_2$	7/3	14/15	6	3/2
$A6_3$	8/3	16/15	6	3/2

Two factors play a role when comparing different genetic alphabets in EarlyWorld. The first one is the connection time, that is, the average number of attempts (or time steps) that a nt takes to find a complementary nt to attach to, which is equal to the alphabet size \mathcal{A} (with the exception of $A4^*$, which allows 3 kinds of base pairs with only 4 letters). The second one is the number of hydrogen bonds involved in each base pair: we now assume that the probability of denaturation of a

dsRNA is proportional to the total number of hydrogen bonds formed between a template and its complementary strand, and not just to the so-far length of the copied molecule. Consequently, the denaturation probability of hybridized dsRNA (Eq. 2) becomes $P = e^{-n\beta/n_{A4}}$, where n represents the number of hydrogen bonds in the molecule and $n_{A4} = 2.5$ is the average number of bonds per nt in the A4 alphabet.

In order to compare the replication efficiency of RNA composed of the 6 different alphabets under study, Fig. 5A shows the dependence of the maximum length of the replicated strand R obtained by EarlyWorld with the oscillation period in an α - and β -sinusoidal environment (with system parameters equivalent to those in Fig. 4B). The absolute maximum in replication length decreases with the alphabet size because of the slowing down of replicative dynamics (i.e., growth of connection time) for large alphabets. The effect related to the dif-

ferent number of hydrogen bonds between complementary nucleotides makes G \equiv C-rich and X \equiv Y-rich dsRNA molecules more robust under denaturations and faster in polymerizing, accelerating the system dynamics and in consequence shifting the curves towards smaller periods (as it can be observed when comparing A2_{gc} vs. A2_{au} and A6₃ vs. A6₂). Remarkably, A4* reaches significantly longer maximum polymer lengths than A4 because of its faster polymerization rate due to the formation of the non-canonical base pair G=U, performing in fact similar to A2_{gc}.

Additionally, if the total number of different ssRNA sequences that can be replicated with a length l of \mathcal{A} nucleotides, \mathcal{A}^l , is used as a proxy for the molecular diversity –or, if preferred, information storage capacity– associated with a population of polymers of a certain genetic alphabet, Fig. 5B shows that A4* represents an optimum combination in terms of diversity and replication speed, its absolute maximum outperforming the rest of alphabets in at least one order of magnitude. In turn, the absolute maximum molecular diversity associated with the canonical four-letter alphabet A4 is two orders of magnitude larger than that of two-letter alphabets, and similar to the much more energetically consuming six-letters ones.

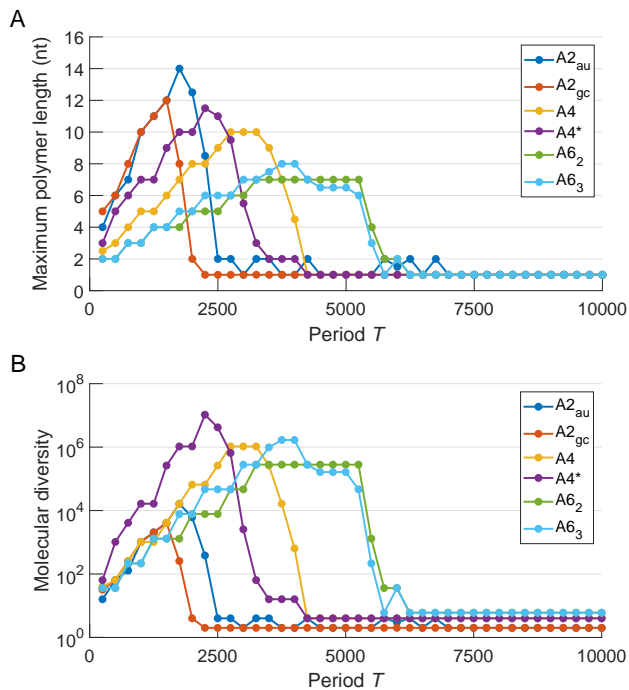


FIG. 5: Efficiency of template-dependent RNA replication is evaluated across six different alphabets. (A) Median of the distribution of maximum R polymer lengths, and (B) median of the molecular diversity computed as \mathcal{A}^l , where \mathcal{A} stands for the alphabet size and l is the median of the distribution of maximum R polymer lengths, for different values of the period $T = T_\alpha = T_\beta$. $\alpha_0 = 0.8$, $A_\alpha = 0.5$ and $\beta_0 = 6$, $A_\beta = 5.9$. Every simulation started with a random 20-nt RNA sequence, and was repeated 100 times.

ferent number of hydrogen bonds between complementary nucleotides makes G \equiv C-rich and X \equiv Y-rich dsRNA molecules more robust under denaturations and faster in polymerizing, accelerating the system dynamics and in consequence shifting the curves towards smaller periods (as it can be observed when comparing A2_{gc} vs. A2_{au}

D. Theoretical approach to RNA replication in EarlyWorld

We propose here a simplified theoretical description of the RNA polymerization and replication process where isolated nts can adsorb to, polymerize on and be released from the clay (level 0 in EarlyWorld, comp.I) or from a ssRNA already adsorbed to the clay (level 1 in EarlyWorld, comp.II). For simplicity, the model entails a unique interaction parameter γ that plays the role of both α and β , depending on the case. It is assumed that the probability P_i of forming and releasing a polymer of length i to the aqueous phase or pool (level 2 in EarlyWorld) is equal to the probability of a single nt of remaining adsorbed to the surface (level 0 in comp.I and level 1 in comp.II) for one time step, receiving a new nt that lands adjacent to it (which we assume with probability 1 for simplicity), remaining the new 2-mer ssRNA adsorbed for one time step, and so on until the polymer reaches length i after i time steps and is released to the pool. In summary, this iterative calculation yields the probability P_i of generating the sequences of length i for any i , in a constant environment, as

$$P_1 = e^{-\gamma}; \quad P_i = e^{-i\gamma} \prod_{k=1}^{i-1} (1 - e^{-k\gamma}) \quad \text{for } 2 \leq i \leq i_{max}, \quad (3)$$

where i_{max} should be large enough to make $P_{i_{max}}$ negligible: $i_{max} = 50$ in all calculations. The mean length of the polymers produced for a given interaction parameter γ is

$$\bar{l} = \sum_{i=1}^{i_{max}} i \cdot P_i, \quad (4)$$

a complex but totally explicit mathematical expression. To model the clay-nt interaction in both comp.I and II

in fluctuating environments, $\gamma = \alpha$ oscillates with time as

$$\gamma = \gamma_0 + A \sin(2\pi i/T), \quad (5)$$

where γ_0 is the average interaction parameter, A is the oscillation amplitude and T the oscillation period. T is an integer number between $T_{min} = 3$ (to avoid $\sin(2\pi i/T) = 0$ for all i) and $T_{max} = i_{max}/2$ (to make sure that the system reproduces at least two full oscillations). Note, however, that the nt-nt interaction in comp.II is influenced by the genetic alphabet in use due to complementary base pairing. In consequence, the evolution of $\gamma = \beta$ in fluctuating environments becomes

$$\gamma = s_{\mathcal{A}}(\gamma_0 + A \sin(2\pi t_{\mathcal{A}} i/T)), \quad (6)$$

where $s_{\mathcal{A}}$ is proportional to the average number of hydrogen bonds between two nts for each alphabet, and $t_{\mathcal{A}}$ is proportional to the connection time that a nt in the pool would take in average to find its complementary one (see Table I).

Fig. 6A plots the dependence of the mean length \bar{l} of the polymers produced by the system on the average interaction parameter γ_0 (i.e., α_0 in comp.I and II and β_0 in comp.II) for a constant environment (given by Eqs. 3-4 with $\gamma = \gamma_0$) and two different oscillating environments (given by Eqs. 3-5 for $\gamma_0 = \alpha_0$ and 3-6 for $\gamma_0 = \beta_0$). All mean polymer lengths show a maximum \bar{l}_{max} for intermediate values of γ_0 , as it happened in the EarlyWorld simulations shown in Figs. 2B and 3A. Note that the maximum of the mean lengths of both oscillating environments are larger than that of the constant one $\bar{l}_{cons} = 1.4823$. In order to verify theoretically whether this is a general behavior, Fig. 6B shows the difference between the maximum of the mean lengths of the polymers produced in oscillating environments and constant environments (i.e., $\bar{l}_{max} - \bar{l}_{cons}$) for an exhaustive range of all the system parameters. This subtraction results to be always positive, proving that oscillatory environments are always more favorable than constant ones regarding the abiotic polymerization and replication of RNA sequences.

Despite the simplicity of this mathematical model in comparison to the EarlyWorld computational environment, it captures several of its main findings, reinforcing its generality. As an example, Fig. 6C shows the dependence of the mean length of the polymers produced by the system with the interaction parameter γ_0 and the oscillation period T , where it is clear that for any meaningful value of the environment (i.e., of the physico-chemical parameters that influence the clay-nt and nt-nt molecular interactions), the system shows the maximum replication efficiency for intermediate values of the period, as it was shown in Fig. 4B for EarlyWorld. Fig. 6D is focused on the influence of the amplitude fraction f , remarking that only strongly oscillatory environments give rise to significant replication dynamics, in agreement with Fig. 4A for the numerical model. Finally, Fig. 6E,F compare the proficiency of 6 genetic alphabets in the polymerization and

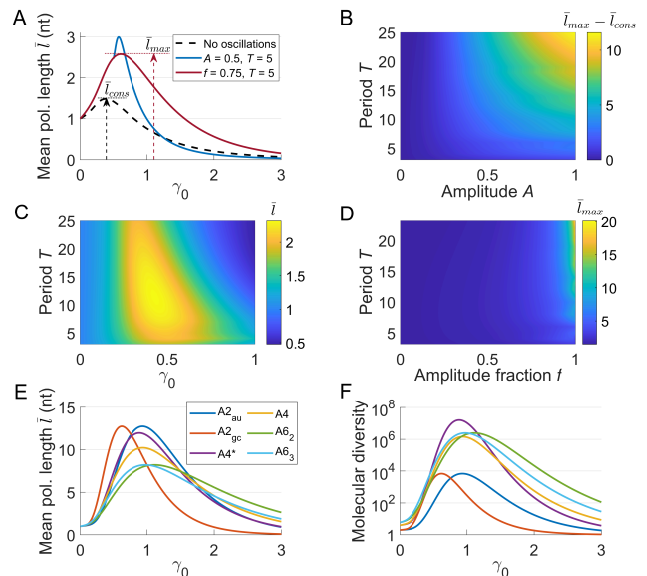


FIG. 6: Simplified mathematical approach to the polymerization and replication of a ssRNA molecule on a clay surface. (A) Dependence of the mean polymer length \bar{l} produced on the average interaction parameter γ_0 in three scenarios: a constant environment ($\gamma = \gamma_0$), an oscillating environment with amplitude $A = 5$ ($\gamma_0 \geq A$ to avoid meaningless negative γ) and period $T = 5$, and an oscillating environment of relative amplitude $f = 0.75$ and $T = 5$. The maximum mean length of the polymers produced in an oscillating environment \bar{l}_{max} and in the constant environment $\bar{l}_{cons} = 1.4823$ are remarked. (B) Difference between the maximum mean length produced in oscillating environments and in the constant environment for an exhaustive range of system parameters. Interestingly, all values of $\bar{l}_{max} - \bar{l}_{cons}$ are > 0 . (C) Dependence of the mean length of polymers produced in oscillating environments \bar{l} with the average interaction parameter γ_0 and the period T , $f = 0.6$. (D) Dependence of the maximum mean length of the polymers \bar{l}_{max} produced in oscillating environments with the amplitude fraction f and the period T . (E) Mean length \bar{l} of the polymers produced in oscillating environments for six different genetic alphabets and a wide range of γ_0 , $f = 0.95$, and $T = 25$. (F) Molecular diversity $\mathcal{A}^{\bar{l}}$ associated with the polymers produced for different genetic alphabets in (E).

replication of primordial RNA molecules. Here the mathematical model recovers precisely the results obtained for EarlyWorld in Fig. 5, as: (i) faster hybridization dynamics of small alphabets (composed of 2 or 4 nts) make them generically outperform large alphabets and (ii) regarding molecular diversity, the absolute maximum of alphabet A4 coincides in performance with any larger alphabet and drastically outperforms 2-letter ones, while A4* shows an unbeatable combination of alphabet length and speed of replication dynamics.

III. DISCUSSION

The transition from astrochemistry to prebiotic chemistry and then to life on Earth involved critical steps toward increasing complexity, with the origin of genetic information and its template-dependent replication being a key unresolved question [71, 72]. Motivated by this challenge, we developed EarlyWorld, a computational model that simulates primordial RNA polymerization and replication, driven solely by the interactions at the clay-water interface. The model features two interconnected compartments within the clay, enabling processes that are difficult to achieve in other heterogeneous, plausibly prebiotic environments, such as lipid-water interfaces and ice-water eutectic phases [1, 52]. The system’s performance depends on two parameters representing the strength of clay-nt (α) and nt-nt (β) interactions. Given that fluctuating, out-of-equilibrium conditions likely played a key role in life’s origins [52], we explored a range of oscillatory patterns by varying α and β both periodically and aperiodically.

Despite random elongation of some RNA sequences, as described in [33], our results indicate that 20-mer RNA oligonucleotides can polymerize efficiently and replicate with a 100% accuracy under specific oscillating environmental conditions (see Fig. S3), whose compatibility across both compartments of the system suggests that all steps of polymerization and replication could occur within a single physical environment. In particular, temperature, pH, salinity, or humidity should fluctuate with (i) large amplitudes (Fig. 4A), and (ii) periods matching the time necessary to polymerize a ssRNA of the same length as the template (Fig. 4B, Fig. S5).

The ability of our model to generate plausible and testable predictions about environments that could optimize primordial RNA replication hinges on result (ii), combined with recent geochemical insights into Hadean Earth conditions [73] and the estimates of template-dependent RNA polymerization times at clay-water interfaces. Though precise experimental data for these polymerization times remain yet unavailable, relevant experiments offer insight. Extensive work by Ferris and collaborators [17, 18, 20, 57] demonstrates that RNA polymerization time on montmorillonite clay varies significantly, depending on nt types, concentrations, presence in their phosphate groups of activating leaving groups, and availability of short RNA primers, ranging from 0.6 to 11 hours per nt [18]. Additionally, nonenzymatic template-dependent RNA polymerization in aqueous solution without mineral substrate yields a polymerization time of approximately 1 h/nt [74–76], which may extend to 1 day/nt under conditions that increase prebiotic plausibility [77]. Considering a hydrolysis time of ~ 20 -50 h/nt [75], which helps us to fix an upper bound, we estimate here a plausible clay-catalyzed template-dependent RNA polymerization time in prebiotic conditions of 1 h/nt to 1 day/nt. As a result, oscillation periods should range from around one (current) day to a few weeks

to support efficient clay-catalyzed replication of ssRNA oligomers long enough to be functional (i.e., > 15 nt) at the dawn of the RNA world.

Recent and precise analyses of tidal interactions in the Earth-Moon system since its formation [73] suggest that the Earth-Moon distance was 50-62% of its current value (Fig. S7A) and that a day lasted about 10-12 h when life emerged on Earth, approximately 4.2-3.8 Gyr ago [3, 62, 63] (Fig. S7B). The oscillation periods required for RNA replication, as discussed earlier, exceed the timescales of daily temperature fluctuations from early Earth’s day-night cycles or tidal wet-dry dynamics, but are shorter than seasonal variations in temperature and humidity. These oscillations, however, align well with spring tides, those maximal tides that occur twice each synodic month (the period between two Sun-Earth-Moon alignments), with a spring tide period of around 125-175 h when life emerged (Fig. S7C). Unlike other potential fluctuating prebiotic scenarios, tidal pools benefit from the strictly periodical behavior of tidal forces, and have already been considered potentially relevant for prebiotic chemistry [53, 54]. These pools would have facilitated interactions between a wide array of reactants carried by rivers, oceans, or the atmosphere [3], on a planet where isotopic evidence from detrital zircons indicates that continental crust may have formed as early as 4.35 Gyr ago [78, 79]. Given that –to first order– tidal amplitudes decrease with the cube of the Earth-Moon and Earth-Sun distances [80], the Moon’s contribution was 4 to 8 times greater than today, while the Sun’s contribution has remained constant, as the Earth-Sun distance has not substantially changed since then. Therefore, every 10-18 early Earth’s days warm seawater would flood dry clay-bottomed ponds covered by salt precipitates, located far enough from the shoreline to be unaffected by daily tides. This seawater influx had three key effects: (i) delivering fresh nts from the sea or nearby sources; (ii) increasing the temperature at clay-water interfaces; and (iii) reducing the local concentration of monovalent and divalent cations. Together, (ii) and (iii) increased the medium’s astringency (i.e., reduced α and β in the EarlyWorld model), weakening nt hydrogen bonding and promoting RNA strand separation. These findings are consistent with the results shown in Fig. 2 of [52], where temperatures above 60°C, Na^+ concentrations below 100 mM, and Mg^{2+} concentrations below 5 mM promote dsRNA denaturation. After several days of no further seawater input, the (perhaps, warm little) pond would dry out again (i.e., increasing α and β in the EarlyWorld model), allowing nts to polymerize on the clay surfaces as well as on the adsorbed ssRNA templates, thus contributing to the overall template-dependent replication. Thanks to the periodic behavior of spring tides, this cyclic process of RNA polymerization and replication could continue without interruption. Fig. S7D presents our model’s prediction for the RNA sequence lengths that would be optimally replicated in a spring tidal pool, based on the polymerization time and the Earth’s time. The range

4-11 h/nt for polymerization times matches the 15-40 nt lengths typically obtained in EarlyWorld. These results encourage experimental efforts to determine precise template-dependent RNA polymerization times in clay-containing prebiotic environments, as they would provide relevant insight into the expected length of primordial RNA oligomers.

In addition, our numerical and theoretical results reveal that the four-letter alphabet with pairing rules [A=U, G≡C, G=U] (A4*, representing current RNA) exhibits superior replication performance than any other alphabet in terms of molecular diversity. The canonical four-letter alphabet [A=U, G≡C] (A4) achieves molecular diversity two orders of magnitude greater than two-letter alphabets, and comparable to the more energetically costly six-letter systems. This strongly supports the primordial selection of four-letter alphabets (especially A4*) for genetic information storage in RNA. Interestingly, A4* introduces sequence mutations through base pair degeneracy (e.g., an A copied as U in the complementary polymer becomes G in the replicated one). While this mutation potential could enhance molecular diversity in early RNA populations, it also risks an error catastrophe (according to quasispecies theory [81]) in case non-canonical base pairs became too prevalent. Actually, G=U interactions are weaker than canonical ones, which may have helped to mitigate this risk.

The precise copies of the original ssRNA produced through the process analyzed in this work should undergo subsequent selection pressures, which recent findings suggest could occur even for 22-nt long oligonucleotides [61]. Studying such selection based on the potential functionality of their molecular structures becomes a promising direction for future research. This will be addressed in the next version of EarlyWorld, thanks to the inclusion of an *in silico* RNA 2D-folding routine [82]. Additional enhancements, such as varying initial nt abundances, differential clay adsorption of purine and pyrimidine nts, allowance for 2'-5' and 5'-5' phosphodiester bonds besides the regioselective formation of 3'-5' ones, consideration of RNA degradation by hydrolysis, and the introduction of replication errors (mismatches, insertions, deletions, and recombination), will help align the computational model more closely with the rules of real (bio)chemistry.

Finally, we have developed a theoretical study of a toy-model of the system that, despite its simplicity, captures several key phenomenological features observed in the computational framework, suggesting the generality of our results beyond specific numerical details. The model highlights the importance of intermediate oscillatory periods and strong fluctuations in nt-nt hydrogen bonding

to facilitate RNA replication, as well as the dominance of four-letter alphabets in a potential primordial soup analogous to that envisioned by A.I. Oparin a century ago. Notably, the model provides rigorous evidence for the enhanced efficiency of RNA polymerization and replication in oscillating environments compared to constant conditions at aqueous-clay interfaces. The Moon's role in providing such oscillations in early Earth may have been crucial for the emergence of heritable information, and suggests that exoplanets with surface liquid water in interaction with clays (or, eventually, other heterogeneous rocks that provide catalytic surfaces) and orbited by large moons could be promising targets in the search for extraterrestrial life.

Acknowledgments

The authors are indebted to B. Corominas-Murtra, A. de la Escosura, M. Fernández-Ruz, and R. Guantes for critical reading of the manuscript; and to J. Aguirre-Becerril, M. Castro, P. Catalán, J.A. Cuesta, J. Irazo, and S. Manrubia for their useful comments. J.A. and C.A. received support from grant No. PID2021-122936NB-I00, C.B. from grant No. PID2022-139908OB-I00 and A.A. from grant No. MDM-2017-0737 Unidad de Excelencia "María de Maeztu" - Centro de Astrobiología (CSIC-INTA), all of them funded by the Spanish Ministry of Science and Innovation/State Agency of Research MCIN/AEI/10.13039/501100011033 and by "ERDF A way of making Europe". C.A. acknowledges the support of the Consejería de Educación, Ciencia y Universidades de la Comunidad de Madrid through grants No. PEJ-2021-AI/TIC-22450 and PIPF-2023/TEC29607 and A.A. the support of the field of excellence Complexity of life in basic research and innovation' of the University of Graz. Authors benefited from the interdisciplinary framework provided by CSIC through the 'LifeHUB.CSIC' initiative (PIE 202120E047-Conexiones-Life).

Author contributions

C.A, A.A, C.B., and J.A. designed the study, conceived the computational environment and wrote the paper; C.A, A.A and J.A. implemented the algorithm; C.A and A.A performed the numerical experiments; J.A. developed the analytical work; and C.B. explored the connections with experimental prebiotic chemistry. The authors declare no conflict of interest.

[1] K. Ruiz-Mirazo, C. Briones, and A. de la Escosura, *Chemical Reviews* **114**, 285 (2014).

[2] J. D. Sutherland, *Angewandte Chemie International Edi-*

tion **55**, 104 (2016).

[3] N. Kitadai and S. Maruyama, *Geoscience Frontiers* **9**, 1117 (2018).

- [4] M. Preiner, S. Asche, S. Becker, H. C. Betts, A. Boniface, E. Camprubi, K. Chandru, V. Erastova, S. G. Garg, N. Khawaja, et al., *Life* **10**, 20 (2020).
- [5] A. I. Oparin, Moscow: Izd. Moskovhii Rabochii (1924).
- [6] J. B. S. Haldane, *Rationalist Annual* **148**, 3 (1929).
- [7] W. Gilbert, *Nature* **319**, 618 (1986).
- [8] M. P. Robertson and G. F. Joyce, *Cold Spring Harbor Perspectives in Biology* **4**, a003608 (2012).
- [9] B. K. Pearce, R. E. Pudritz, D. A. Semenov, and T. K. Henning, *Proceedings of the National Academy of Sciences* **114**, 11327 (2017).
- [10] J. W. Szostak, *Philosophical Transactions of the Royal Society B: Biological Sciences* **366**, 2894 (2011).
- [11] G. F. Joyce and J. W. Szostak, *Cold Spring Harbor Perspectives in Biology* **10**, a034801 (2018).
- [12] O. Leslie E, *Critical Reviews in Biochemistry and Molecular Biology* **39**, 99 (2004).
- [13] W. K. Johnston, P. J. Unrau, M. S. Lawrence, M. E. Glasner, and D. P. Bartel, *Science* **292**, 1319 (2001).
- [14] X. Portillo, Y.-T. Huang, R. R. Breaker, D. P. Horning, and G. F. Joyce, *Elife* **10**, e71557 (2021).
- [15] N. Papastavrou, D. P. Horning, and G. F. Joyce, *Proceedings of the National Academy of Sciences* **121**, e2321592121 (2024).
- [16] I. A. Chen, *Proceedings of the National Academy of Sciences* **121**, e2402649121 (2024).
- [17] W. Huang and J. P. Ferris, *Chemical Communications* pp. 1458–1459 (2003).
- [18] W. Huang and J. P. Ferris, *Journal of the American Chemical Society* **128**, 8914 (2006).
- [19] J. T. Klopogge and H. Hartman, *Life* **12**, 259 (2022).
- [20] J. P. Ferris, *Philosophical Transactions of the Royal Society B: Biological Sciences* **361**, 1777 (2006).
- [21] C. A. Jerome, H.-J. Kim, S. J. Mojzsis, S. A. Benner, and E. Biondi, *Astrobiology* **22**, 629 (2022).
- [22] S. Himbert, M. Chapman, D. W. Deamer, and M. C. Rheinstädter, *Scientific Reports* **6**, 31285 (2016).
- [23] J. Attwater, A. Wochner, V. B. Pinheiro, A. Coulson, and P. Holliger, *Nature Communications* **1**, 76 (2010).
- [24] C. Briones, M. Stich, and S. C. Manrubia, *RNA* **15**, 743 (2009).
- [25] F. Wachowius and P. Holliger, *ChemSystemsChem* **1**, 1 (2019).
- [26] C. Deck, M. Jauker, and C. Richert, *Nature Chemistry* **3**, 603 (2011).
- [27] K. Adamala and J. W. Szostak, *Science* **342**, 1098 (2013).
- [28] K. Adamala, A. E. Engelhart, and J. W. Szostak, *Journal of the American Chemical Society* **137**, 483 (2015).
- [29] D. K. O’Flaherty, L. Zhou, and J. W. Szostak, *Journal of the American Chemical Society* **141**, 10481 (2019).
- [30] P. W. Anderson, *Proceedings of the National Academy of Sciences* **80**, 3386 (1983).
- [31] D. S. Rokhsar, P. Anderson, and D. Stein, *Journal of Molecular Evolution* **23**, 119 (1986).
- [32] L. E. Orgel, *Nature* **358**, 203 (1992).
- [33] C. Fernando, G. Von Kiedrowski, and E. Szathmáry, *Journal of Molecular Evolution* **64**, 572 (2007).
- [34] A. V. Tkachenko and S. Maslov, *The Journal of Chemical Physics* **143** (2015).
- [35] H. Fellermann, S. Tanaka, and S. Rasmussen, *Physical Review E* **96**, 062407 (2017).
- [36] S. Toyabe and D. Braun, *Physical Review X* **9**, 011056 (2019).
- [37] A. S. Tupper and P. G. Higgs, *Journal of Theoretical Biology* **527**, 110822 (2021).
- [38] J. H. Rosenberger, T. Göppel, P. W. Kudella, D. Braun, U. Gerland, and B. Altaner, *Physical Review X* **11**, 031055 (2021).
- [39] L. Zhou, D. Ding, and J. W. Szostak, *RNA* **27**, 1 (2021).
- [40] J. Juritz, J. M. Poulton, and T. E. Ouldrige, *The Journal of Chemical Physics* **156** (2022).
- [41] S. I. Walker, M. A. Grover, and N. V. Hud, *PLOS ONE* **7**, e34166 (2012).
- [42] H. Kaddour and N. Sahai, *Life* **4**, 598 (2014), ISSN 2075-1729, URL <https://www.mdpi.com/2075-1729/4/4/598>.
- [43] C. B. Mast, S. Schink, U. Gerland, and D. Braun, *Proceedings of the National Academy of Sciences* **110**, 8030 (2013).
- [44] M. Kreysing, L. Keil, S. Lanzmich, and D. Braun, *Nature Chemistry* **7**, 203 (2015).
- [45] G. Costanzo, S. Pino, F. Ciciriello, and E. Di Mauro, *Journal of Biological Chemistry* **284**, 33206 (2009).
- [46] M. Morasch, C. B. Mast, J. K. Langer, P. Schilcher, and D. Braun, *ChemBioChem* **15**, 879 (2014).
- [47] N. Lahav, D. White, and S. Chang, *Science* **201**, 67 (1978).
- [48] V. Kompanichenko, *Origins of Life and Evolution of Biospheres* **42**, 153 (2012).
- [49] B. Damer and D. Deamer, *Life* **5**, 872 (2015).
- [50] H. Kaddour, S. Gerislioglu, P. Dalai, T. Miyoshi, C. Wesdemiotis, and N. Sahai, *The Journal of Physical Chemistry C* **122**, 29386 (2018).
- [51] F. Senatore, R. Serra, and M. Villani, in *Artificial Life and Evolutionary Computation* (Springer, Cham, 2023), pp. 119–129, ISBN 978-3-031-31183-3.
- [52] A. Ianeselli, A. Salditt, C. Mast, B. Ercolano, C. L. Kufner, B. Scheu, and D. Braun, *Nature Reviews Physics* **5**, 185 (2023).
- [53] R. Lathe, *Icarus* **168**, 18 (2004).
- [54] R. Lathe, *International Journal of Astrobiology* **4**, 19 (2005).
- [55] J. W. Szostak, *Journal of Systems Chemistry* **3**, 1 (2012).
- [56] A. Ianeselli, M. Atienza, P. W. Kudella, U. Gerland, C. B. Mast, and D. Braun, *Nature Physics* **18**, 579 (2022).
- [57] J. P. Ferris, A. R. Hill Jr, R. Liu, and L. E. Orgel, *Nature* **381**, 59 (1996).
- [58] M. F. Aldersley, P. C. Joshi, J. D. Price, and J. P. Ferris, *Applied Clay Science* **54**, 1 (2011).
- [59] S. Jelavić, D. Tobler, T. Hassenkam, J. J. De Yoreo, S. Stipp, and K. K. Sand, *Chemical Communications* **53**, 12700 (2017).
- [60] J. B. Swadling, P. V. Coveney, and H. C. Greenwell, *Journal of the American Chemical Society* **132**, 13750 (2010).
- [61] G. Bartolucci, A. Calaça Serrão, P. Schwintek, A. Kühnlein, Y. Rana, P. Janto, D. Hofer, C. B. Mast, D. Braun, and C. A. Weber, *Proceedings of the National Academy of Sciences* **120**, e2218876120 (2023).
- [62] E. R. R. Moody, S. Álvarez Carretero, T. A. Mahendrarajah, J. W. Clark, H. C. Betts, N. Dombrowski, L. L. Szánthó, R. A. Boyle, S. Daines, X. Chen, et al., *Nature Ecology & Evolution* **8665**, 1654 (2024), URL <https://doi.org/10.1038/s41559-024-02461-1>.
- [63] B. K. Pearce, A. S. Tupper, R. E. Pudritz, and P. G. Higgs, *Astrobiology* **18**, 343 (2018).
- [64] F. Macht, K. Eusterhues, G. J. Pronk, and K. U. Totsche, *Applied Clay Science* **53**, 20 (2011).
- [65] J. Lipfert, G. M. Skinner, J. M. Keegstra, T. Hensgens,

- T. Jager, D. Dulin, M. Köber, Z. Yu, S. P. Donkers, F.-C. Chou, et al., *Proceedings of the National Academy of Sciences* **111**, 15408 (2014).
- [66] V. Ervithayasuporn, S. Chanmungkalakul, N. Churinthorn, T. Jaroentomeechai, S. Hanprasit, R. Sodkhomkhum, P. Kaewpijit, and S. Kiatkamjornwong, *Applied Clay Science* **171**, 6 (2019).
- [67] P. J. Flory, *Principles of polymer chemistry* (Cornell university press, 1953).
- [68] P. Svoboda and A. D. Cara, *Cellular and Molecular Life Sciences CMLS* **63**, 901 (2006).
- [69] E. Szathmáry, *Proceedings of the Royal Society of London. Series B: Biological Sciences* **245**, 91 (1991).
- [70] E. Szathmáry, *Nature Reviews Genetics* **4**, 995 (2003).
- [71] E. Szathmáry and J. M. Smith, *Nature* **374**, 227 (1995).
- [72] M. García-Sánchez, I. Jiménez-Serra, F. Puente-Sánchez, and J. Aguirre, *Proceedings of the National Academy of Sciences* **119**, e2119734119 (2022), <https://www.pnas.org/doi/pdf/10.1073/pnas.2119734119>, URL <https://www.pnas.org/doi/abs/10.1073/pnas.2119734119>.
- [73] M. Farhat, P. Auclair-Desrotour, G. Boué, and J. Laskar, *Astronomy & Astrophysics* **665**, L1 (2022), URL <https://doi.org/10.1051/0004-6361/202243445>.
- [74] T. Wu and L. E. Orgel, *Journal of the American Chemical Society* **114**, 317 (1992).
- [75] J. C. Blain and J. W. Szostak, *Annual Review of Biochemistry* **83**, 615 (2014).
- [76] L. Li, N. Prywes, C. P. Tam, D. K. O’flaherty, V. S. Lelyveld, E. C. Izgu, A. Pal, and J. W. Szostak, *Journal of the American Chemical Society* **139**, 1810 (2017).
- [77] D. Ding, L. Zhou, S. Mittal, and J. W. Szostak, *Journal of the American Chemical Society* **145**, 7504 (2023).
- [78] T. M. Harrison, A. K. Schmitt, M. T. McCulloch, and O. M. Lovera, *Earth and Planetary Science Letters* **268**, 476 (2008), ISSN 0012-821X, URL <https://www.sciencedirect.com/science/article/pii/S0012821X08000897>.
- [79] E. E. Stüeken, R. E. Anderson, J. S. Bowman, W. J. Brazelton, J. Colangelo-Lillis, A. D. Goldman, S. M. Som, and J. A. Baross, *Geobiology* **11**, 101 (2013), <https://onlinelibrary.wiley.com/doi/pdf/10.1111/gbi.12025>, URL <https://onlinelibrary.wiley.com/doi/abs/10.1111/gbi.12025>.
- [80] G. J. MacDonald, *Reviews of Geophysics* **2**, 467 (1964).
- [81] M. Eigen and P. Schuster, *Naturwissenschaften* **65**, 7 (1978).
- [82] R. Lorenz, S. H. Bernhart, C. H. zu Siederdissen, H. Tafer, C. Flamm, P. F. Stadler, and I. L. Hofacker, *Algorithms for Molecular Biology* **6**, 26 (2011), URL <http://eprints.cs.univie.ac.at/3262/>.

Supporting Information for: Polymerization and replication of primordial RNA explained by clay-water interface dynamics

S1. EarlyWorld’s algorithm

A. Definitions and basic rules of the model

EarlyWorld is a computational environment that simulates, in a simplified, stochastic and discrete-time manner, the non-enzymatic polymerization and template-dependent replication of RNA on a clay-water interface. More precisely, ribonucleotides (nts), single stranded (ss) and double stranded (ds) RNA molecules move from an aqueous solution (the pool from now on) to the surface of a clay, and vice versa. There is a total absence of catalytic molecules such as ribozymes or protein enzymes (e.g., RNA polymerases). Also, ssRNA molecules are not allowed to auto-hybridize forming secondary structures, and they always maintain the orientation when interacting with the clay or another molecule, i.e., they do not turn around (UGA molecule cannot be reattached as AGU, for example). Additionally, any genetic alphabet can be defined in EarlyWorld by the number of different nts and its base-pairing rules.

Dynamics in EarlyWorld takes place in two separated compartments, comp.I and comp.II, each of them representing a different microenvironment of the clay-water interface [1–4], and whose simulations run independently. Three levels are relevant for the evolution of the system: the clay or level 0, where nts and polymers can be adsorbed –described by a 1D-vector of length L – (both in comp.I and comp.II); the complementary level or level 1, where nts can only be placed if they are complementary to those of the template ssRNA placed in level 0 and contribute to the formation of dsRNA molecules via hydrogen bonding –described by a 1D-vector of length L – (only in comp.II); and the aqueous phase, pool or level 2, represented by a *disordered box* where an unlimited number of free nts, ssRNA and dsRNA molecules stay in solution (both in comp.I and comp.II, dsRNA molecules only in the latter).

The system’s performance depends on two main parameters: α describes the strength of the clay-nt interactions –known to be ionic bonds and weak Van der Waal forces [3, 5, 6]–, and β describes the strength of nt-nt interactions –due to hydrogen bonding between nucleobases– [7]. Both quantities depend on the environment that surrounds them.

Simulations in compartments I and II start with a fixed number N of initial nts floating freely in the pool. Unless said otherwise, a clay of length $L = 200$ positions was used (a length sufficiently large to accommodate several small RNA oligomers, while keeping simulations computationally affordable) and an alphabet of four different nts (A4) displaying the canonical base-pairing rules (A=U and G≡C), with $N = 1600$ nts equally distributed between A, U, G and C, so that their abundances were not a limiting factor. Simulations stop when the simulation time t_{max} is reached. Throughout the calculations in this work, $t_{max} = 2 \times 10^4$ except when the dependence of the system on the simulation time is particularly studied (see Fig. S3).

The steps of the algorithm at each time step are similar in both compartments and are summarized as follows:

- A molecule (nt, ssRNA or dsRNA, the latter only in comp.II) selected from the pool falls into the clay.
- Attending to the rules described below in sections S1.B and S1.C, the molecule either (i) remains adsorbed to the clay (level 0), (ii) is hybridized to other nt or ssRNA if they are complementary (level 1, only in comp.II), or (iii) returns to the pool (level 2) with no changes. In the case it remains attached to level 0 or 1, either random or template-dependent polymerization can occur, respectively.
- The breakage probability of all the existing non-covalent interactions in the system (desorption probability in clay-nt interactions and denaturation probability in nt-nt interactions) in that time step is evaluated. As a consequence, some molecules may be released from levels 0 or 1 and return to level 2 (the pool).
- The simulation is repeated t_{max} time steps, and then stops.

B. Detailed description of compartment I simulations

Comp.I represents a clay internal channel or interlayer that is wide enough to accommodate ssRNA molecules, but not dsRNA molecules. Here, random polymerization of nts takes place due to the catalytic action of the clay, but complementary base pairing between nts is not possible.

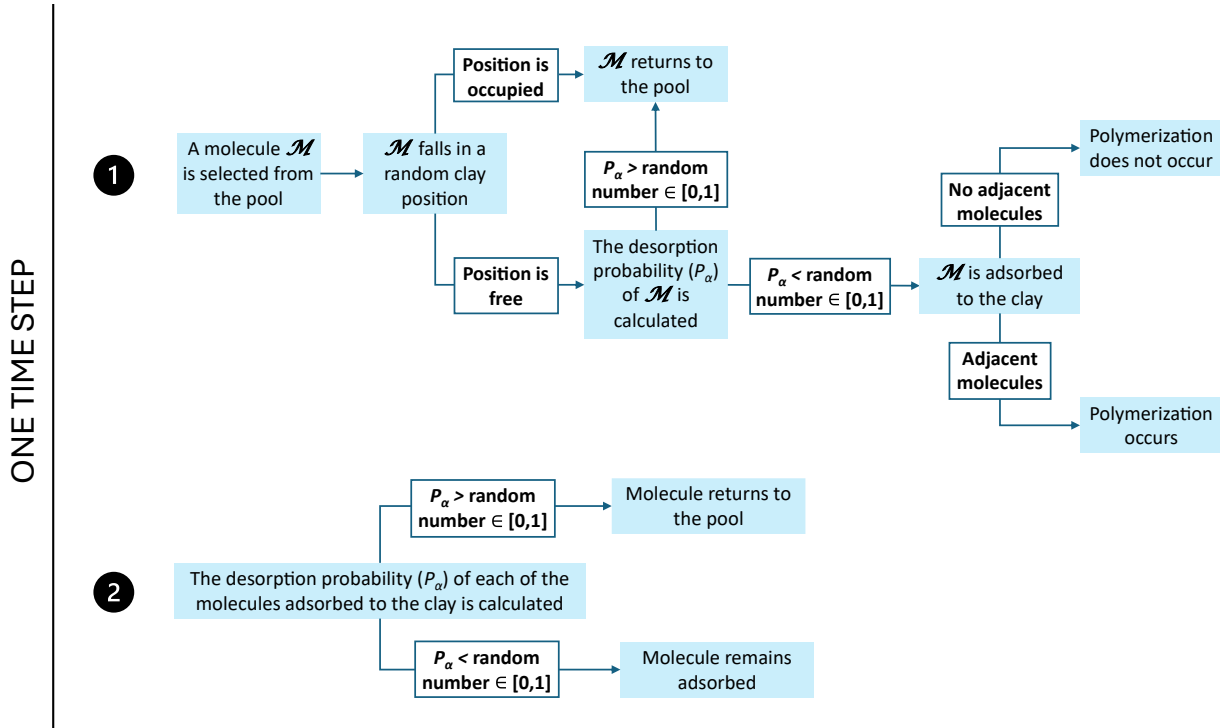


Figure S1: Flow diagram of compartment I simulations. The chart describes the steps followed by the computational algorithm for every time step of a simulation. Two major processes take place in each time step: 1) The dynamics of the molecule \mathcal{M} that falls into the clay, and 2) the dynamics of the rest of nts and ssRNA molecules that are attached to the clay.

Simulations start with N initial nts floating in the pool, as described in section S1.A, and the clay level completely empty. At each time step of the simulation, the system follows the steps depicted in the flow diagram on Fig. S1. As time passes, ssRNA polymers are formed on the clay, desorb and move to the pool (thus enriching it in larger oligomers), and can also be adsorbed again on the clay surface and continue polymerizing. Simulations stop when the simulation time t_{max} is reached. Besides the detailed flow chart of Fig. S1, important considerations are clarified below:

- The molecule \mathcal{M} (that can be a nt or a ssRNA oligomer) selected at time step k to interact with the clay is chosen randomly from all the molecules in the pool with the weighted probability

$$P_k(\mathcal{M}) = \text{length}(\mathcal{M})/S_k, \quad (1)$$

where S_k is the sum of all molecule lengths (computed as their number of nts) present in the pool in time step k . Therefore, larger polymers have more chances to be adsorbed to the clay, as we assume they diffuse slower and remain closer to the clay than smaller oligomers.

- A randomly chosen nt of the selected molecule interacts with a randomly chosen empty position of the clay. The number of positions in the clay that interact with the falling molecule is equal to its length.
- The place on the clay where \mathcal{M} falls is considered empty only if all the individual positions with which the molecule interacts are empty and the whole molecule falls inside the boundaries of the L clay positions.
- P_α is the desorption probability and is calculated as

$$P_\alpha = e^{-l\alpha}, \quad (2)$$

where l stands for the polymer's length (l) and $\alpha > 0$ describes the strength of the clay-nt interactions in the environment that surrounds them. Note that the ssRNA oligomers are attached or detached from the clay along their entire length: this model does not consider partially adsorbed/desorbed molecules. In consequence, Eq. 2 can be interpreted as a Bernoulli random process, where the polymer desorbs from the clay only if all outcomes are successful.

- If polymerization occurs, \mathcal{M} forms a covalent bond with one nt at any of its two adjacent positions (i.e., its 5' or 3' end), producing a longer polymer that is yet attached to the clay until its desorption probability is again evaluated. Throughout the entire simulation, the covalent sugar-phosphate backbone of the polymers remains unbreakable (i.e., RNA hydrolysis is not considered in this model).

C. Detailed description of compartment II simulations

Comp.II represents wide clay channels that can accommodate both ssRNA and dsRNA molecules, as well as inter-particle sites and external clay surfaces. Therefore, here both random polymerization of nts (as in comp.I) and template-dependent RNA replication can occur.

Simulations start with an initial ssRNA of 20 nt in length that represents a polymer formerly produced in comp.I, which has been pushed out of it to eventually enter comp.II, and has finally been adsorbed to its clay. The composition and sequence of this original polymer (strand O from now on) is set randomly at the beginning of each simulation, as well as the clay position of comp.II where it is initially adsorbed. The rest of the initial conditions are the same as in comp.I: simulations start with N initial nts floating in the pool and the clay level completely empty except for the initial O polymer.

At each time step of the simulation, the system follows the flow diagram shown in Fig. S2. As time passes, polymers form and the pool becomes enriched in larger molecules (both ssRNA and dsRNA molecules), that can also be adsorbed again to the clay or, only in the case of ssRNA, be hybridized to other ssRNA at the complementary level or level 1. RNA molecules can form by random polymerization on the clay surface (as it happens in comp.I), but also by template-dependent polymerization (exclusive of comp.II). Thus, during each simulation, the dynamics produces complementary C and replicate R (i.e., complementary of C) strands of the original O, as well as other newly-generated random sequences O_{new} than can also be copied in their complementary C_{new} and replicate R_{new} strands. Only C and R strands of the original O are plotted in the figures of this work, as C_{new} and R_{new} do not proceed from the original ssRNA oligomer O. Finally, simulations stop after t_{max} time steps.

Besides the detailed flow chart of Fig. S2, important considerations are clarified below:

- The molecule \mathcal{M} (which can be a nt, a ssRNA or a dsRNA) selected in the pool and the position of the clay (levels 0 or 1) where it adsorbs are chosen in the same way as in comp.I, section S1.B. When dsRNA molecules are formed, their length (used to compute $P_k(\mathcal{M})$ in Eq. 1) is calculated as the sum of the lengths of the two strands that compose the duplex.
- In comp.II, nts and ssRNA molecules can be adsorbed to the clay (level 0) or be hybridized to a template strand (level 1), the latter happening only if they are fully complementary (mutations or nucleotide mismatches are not accepted in this model). On the contrary, dsRNA molecules can exclusively be adsorbed to the clay (level 0).
- As in comp.I, the place where \mathcal{M} adsorbs is considered empty only if all the positions where the molecule falls (in level 0 or in level 1, depending on the case) are empty and the whole oligomer fits inside the boundaries of the L positions.
- The desorption probability is calculated as in comp.I, Eq. 2.
- The denaturation probability P_β is

$$P_\beta = e^{-l\beta}, \quad (3)$$

where l stands for the dsRNA length and $\beta > 0$ describes the strength of nt-nt interactions in the environment that surrounds them. As it happened with ssRNA molecules adsorbed/desorbed from the clay, ssRNA molecules hybridize and denature from the templates along their entire length: molecules partially hybridized/denatured are not allowed. In consequence, Eq. 3 can also be interpreted as a Bernoulli random process, where the ssRNA denatures from the template only if all outcomes are successful.

- Polymerization occurs as explained for comp.I, section S1.B, but in this case it can take place at both levels: 0 or 1, the latter being a template-dependent polymerization.

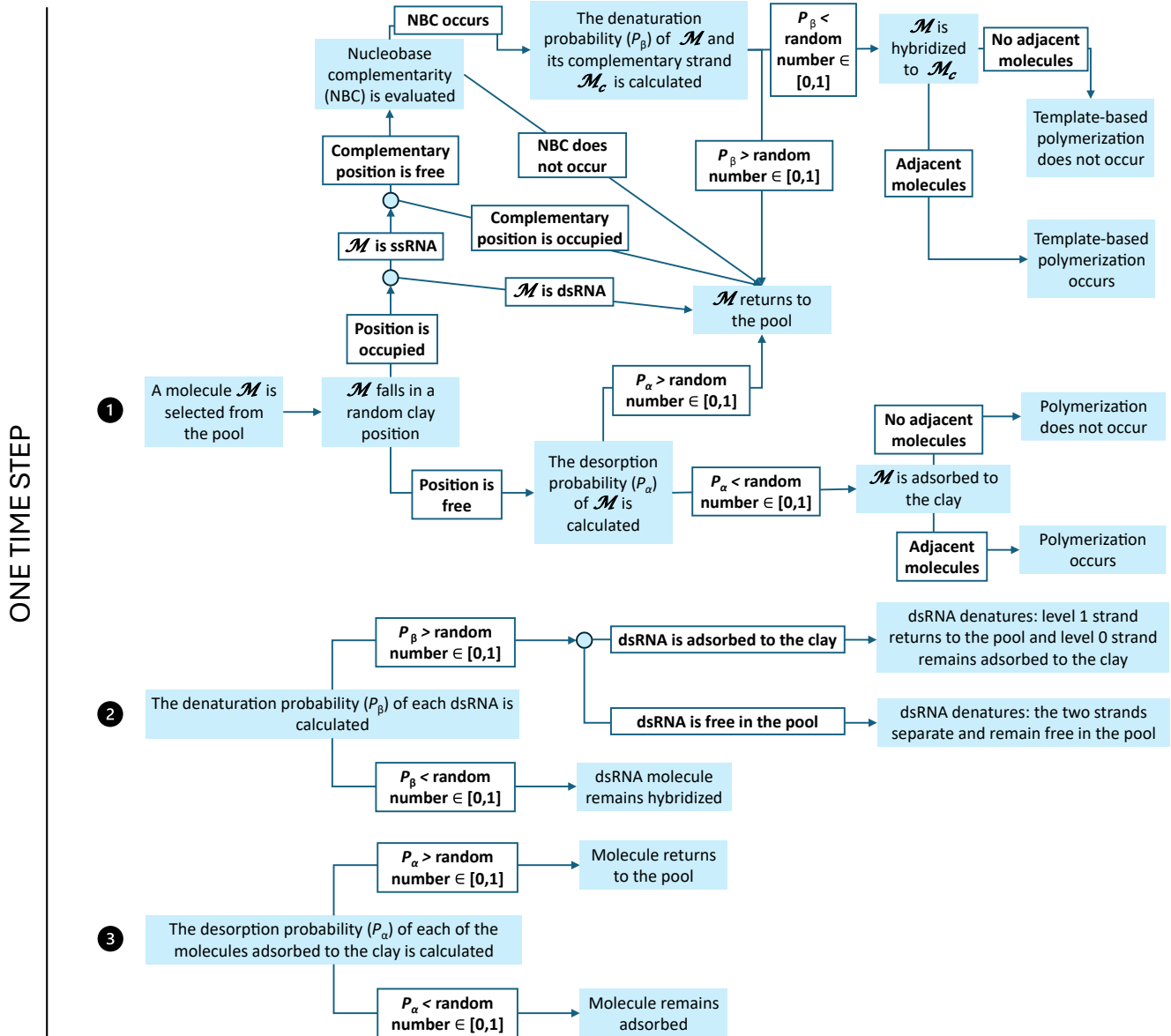


Figure S2: Flow diagram of compartment II simulations. The chart describes the steps followed by the computational algorithm for every time step of a simulation. Three major processes take place in each time step: 1) The dynamics of the molecule \mathcal{M} that is adsorbed to the clay, 2) the dynamics of all the dsRNA molecules both attached to the clay and floating in the pool (in this case, whether they remain hybridized or denature), and 3) the dynamics of all the nts, ssRNA and dsRNA molecules that are attached to the clay (whether they remain adsorbed or they desorb and return to the pool).

S2. Algorithm availability

For further insight on the algorithm, a Matlab(R2020b) implementation with description, documentation and instructions of use is available at the following public repository: <https://github.com/c-alejandrev/EarlyWorld>.

S3. Calculation of maximum polymer lengths

All the computational results displayed in the main text represent statistical measures of the distribution of maximum polymer lengths obtained along every realization for a concrete number of realizations (typically 100), each of them running for a limited number of time steps t_{max} . Simulations are stochastic, therefore each of them represents a different trajectory and, in the case of comp.II, the original ssRNA sequence of 20 nts in length is randomly created at the beginning of every realization.

In comp.I, the maximum polymer length measured in one realization of the process represents the longest polymer formed by adsorption of nts on the clay, which is later on released to the pool at any time step. Notice that even longer polymers attached to the clay may form, but will not be considered until they are detached from the surface.

In comp.II, the maximum polymer lengths measured in one realization of the process are calculated as the lengths of the longest complementary C and replicate R polymers denatured from their templates and released to the pool at any time step. Take into account that if these molecules, additionally to the accurate copy of the corresponding template, have other random or spurious sequences attached to their 5' or 3' ends, the latter will not contribute to the measured length (see section S4).

S4. Sequence accuracy

Complementary C and replicate R molecules of the original O sequence can be “contaminated” at their 5' and/or 3' ends with other added nts or ligated ssRNA molecules, as RNA ligation (either produced –randomly– at level 0 or –in a template-dependent manner– at level 1) is based on the same process of phosphodiester bond formation that is involved in RNA polymerization. As a result, C or R molecules are frequently found to be elongated with random sequences covalently linked to their ends, which are not related to the original molecule O and give rise to chimeric sequences [8]. In order to measure this phenomenon, we define the accuracy of a sequence s of type C or R of length l_s as

$$A_s = 100 \times \frac{l_O}{l_s}, \quad (4)$$

where l_O is the number of nts of sequence s that are (i) complementary to a fraction (or the totality) of the original sequence O in a ssRNA of type C, or (ii) equal to a fraction (or the totality) of the original sequence O in a ssRNA of type R.

To avoid the loss of identity of the original O sequences, the C and R molecules resulting from simulations are only counted if they have an accuracy of $> 75\%$, i.e., their sequences must be formed by $> 75\%$ of products of the copied polymer O. In practice, this means that each replicated ssRNA molecule can be up to 33% longer than the product of the original O it contains. As in the model RNA polymers cannot be degraded or split into shorter oligomers, such additional nts that are allowed to decrease the accuracy of the copied molecule up to 75% appear at its 5' or 3' ends but not at internal positions of the sequence.

For the sake of clarity, we provide here an example of the meaning of the accuracy of a sequence in EarlyWorld: when a simulation in comp.II produces a maximum length of an R molecule equal to 20 nts, with accuracy of $> 75\%$, it means that the replicated sequence has a core of 20 nts that is an exact copy of the original O, but it can show up to 6 spurious nts covalently bound to its 5' or 3' ends (i.e., $20 \leq l_s \leq 26$ nts). In turn, an accuracy of 100% means that R is 20 nts long and its sequence is identical to that of O.

Fig. S3 shows the maximum C (green) and R (purple) polymer length distributions for different simulation times t_{max} , with an accuracy of $> 75\%$ (i.e. the accuracy allowed in this work) in Fig. S3A, and of 100% in Fig. S3B. Importantly, EarlyWorld yields fully accurate (i.e., 100%) C and R sequences of length 20 –and therefore R being identical to O– for certain sets of parameters, although their abundance is, obviously, smaller than that of less accurate polymers.

Finally, note that the efficiency of the results obtained saturate beyond a simulation time of $t_{max} \sim 2 \cdot 10^4$ time steps for an accuracy of $> 75\%$. For this reason, we chose such value for the simulations developed in this work.

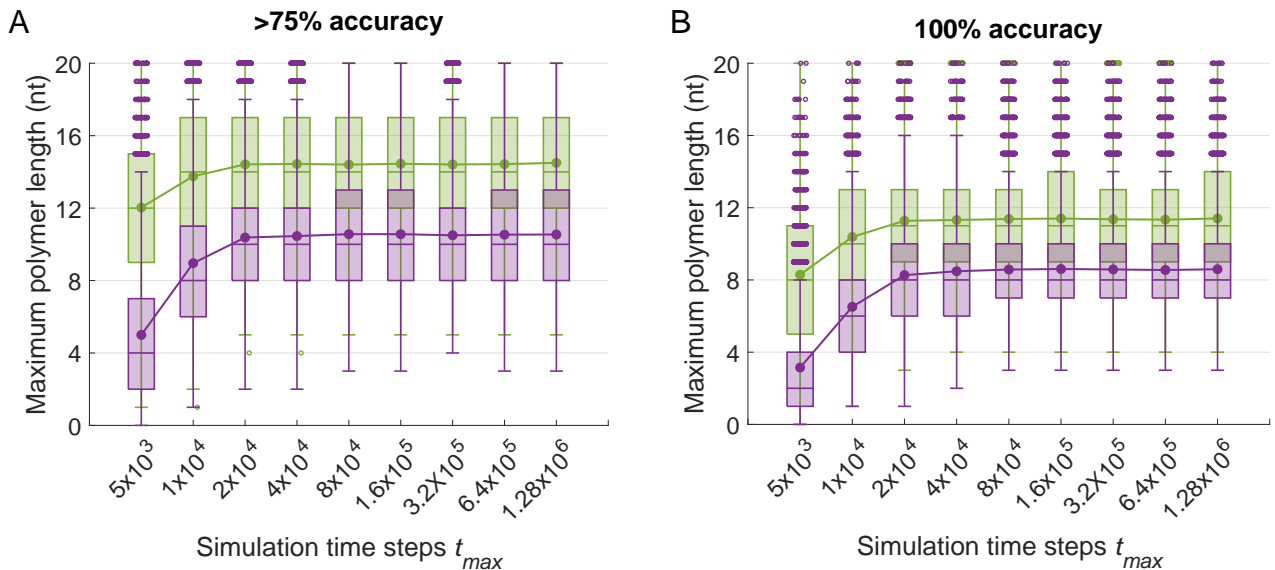


Figure S3: Maximum complementary (C, green) and replicate (R, purple) polymer lengths for different simulation times. Panel (A) plots replication products with an accuracy of $> 75\%$, whereas panel (B) shows products with an accuracy of 100% . Every simulation was repeated 10^4 times. Parameters: $\alpha_0 = 0.6$, $T_\alpha = 2500$, $\beta_0 = 7$, $f = 0.99$ and $T_\beta = 2500$ (coinciding with the most favorable result in Fig. 4A). Note that throughout the paper simulation times were $t_{max} = 2 \times 10^4$ time steps.

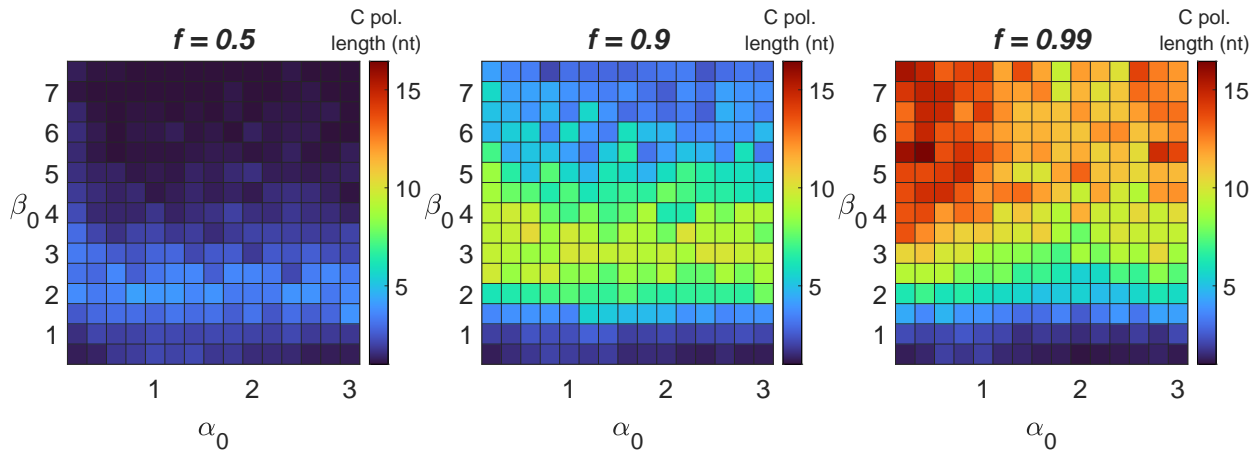


Figure S4: Dependence of the mean of maximum C polymer lengths with average interaction parameters α_0 and β_0 at three different amplitude fractions f (being $A_\alpha = f\alpha_0$ and $A_\beta = f\beta_0$). $T_\alpha = T_\beta = 2500$. Every simulation started with a different 20 nt-long ssRNA molecule of random position and sequence, and means were calculated over 20 independent realizations for each parameter set.

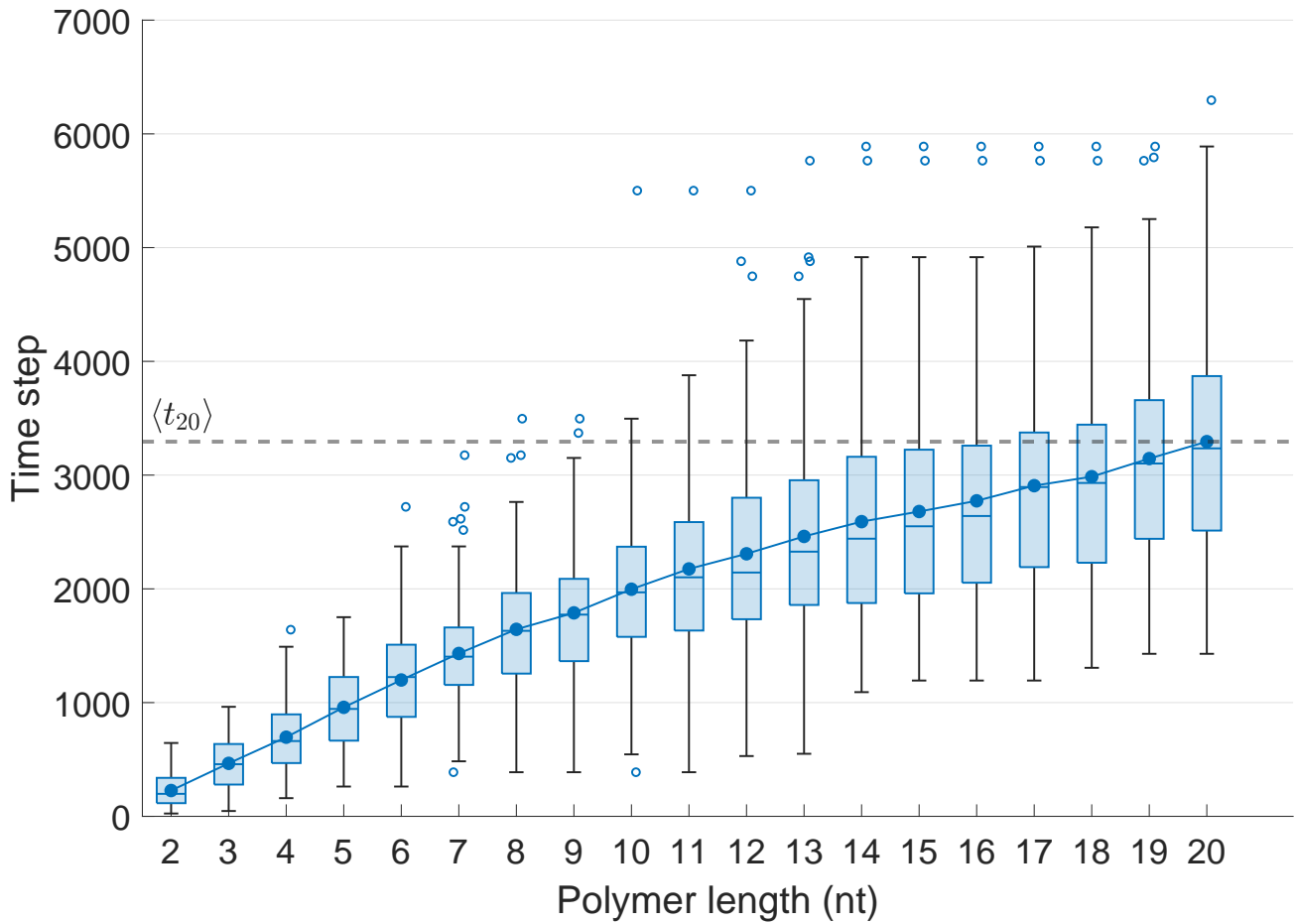


Figure S5: Number of time steps required by EarlyWorld to produce a ssRNA polymer C complementary of the original one (O), by template-dependent polymerization, as a function of its length. In particular, we measure the time step in which a polymer C of a given length appears for the first time hybridized to O in the simulation (i.e., it does not need to be released to the pool). The dashed line shows the mean time $\langle t_{20} \rangle = 3294$ time steps to form a 20-nt long polymer C. Each box plot and mean (colored circles) were calculated using 100 independent realizations. Parameters: $\alpha_0 = 0.8$, $A_\alpha = 0.5$, $T_\alpha = 2500$, $\beta_0 = 6$, $A_\beta = 0$, $T_\beta = 0$.

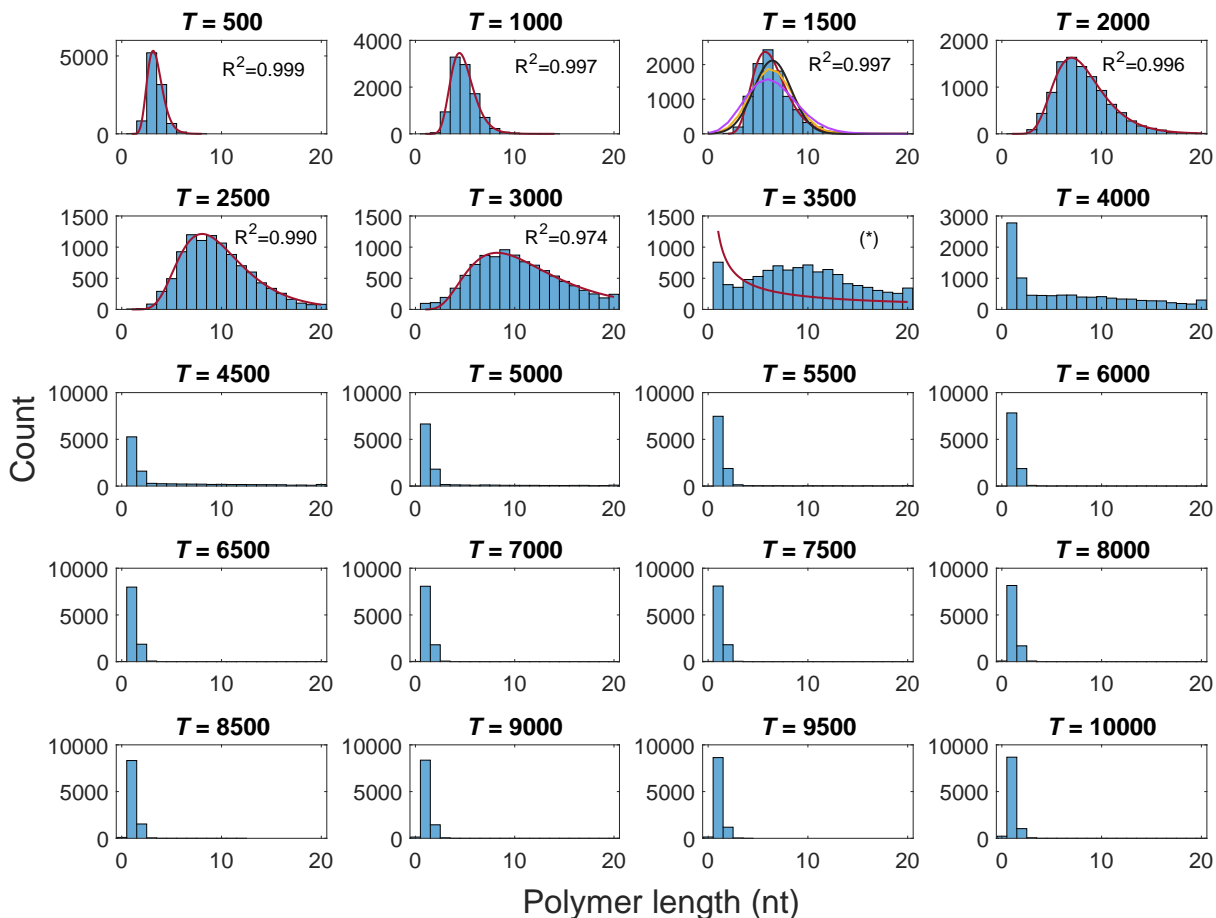


Figure S6: Distribution of maximum R polymer lengths for twenty different oscillation periods $T = T_\alpha = T_\beta$. Approximations to log-normal distributions are displayed in red with their corresponding R^2 coefficient. In $T = 1500$ data were also approximated to a normal distribution (black line, $R^2 = 0.941$), a binomial distribution (yellow line, $R^2 = 0.933$) and a Poisson distribution (pink line, $R^2 = 0.859$). The log-normal distribution approximates accurately the data until a transition occurs at $T \approx 3500$, beyond which the distributions show first a peak in 1 nt and a long tail, and for larger values of T they finally collapse to the absence of any relevant replication. Data include 10^4 independent realizations for each parameter set with parameters $\alpha_0 = 0.8$, $A_\alpha = 0.5$, $\beta_0 = 6$, and $A_\beta = 5.9$ (coinciding with those of Fig. 4B). (*) The log-normal approximation of these data is worse than if they were approximated to a horizontal line.

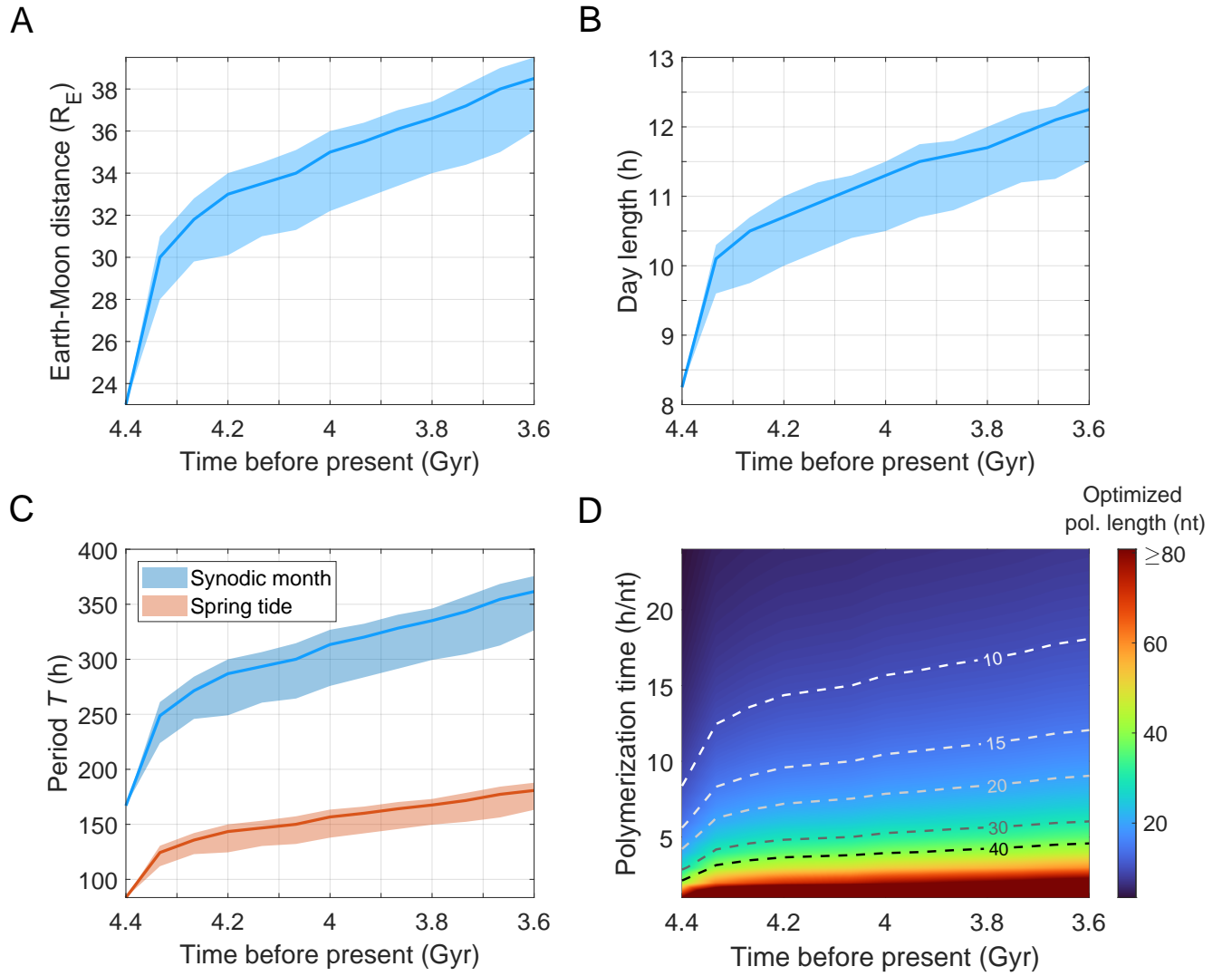


Figure S7: Evolution with time of the main astronomical data related to the Earth-Moon system (panels A,B,C), and dependence of the optimized polymer length on the template-dependent polymerization time in the clay-water scenario considered in early Earth (panel D). (A) Lunar semi-major axis (measured in Earth radii R_E). For comparison, current lunar semi-major axis is $\sim 60R_E$. Data in (A, B) were obtained from Fig. 3 and Fig. 5 in [9]. Bold lines in (A,B,C) represent data means and shaded envelopes correspond to 2σ -uncertainties. (B) Earth's length of the day. (C) Synodic month period (or lunation, or Moon phase cycle, i.e., the time between two Sun-Earth-Moon alignments, calculated applying Kepler's third law to data in panel (A) and current data, blue), and spring tide period T_{st} (i.e., the time between a Sun-Earth-Moon and a Sun-Moon-Earth alignment, orange). Current synodic month period is 29.53 days (708.72 h) and current spring tide period is 14.76 days (354.36 h, half a synodic month). (D) Dependence of the optimized polymer length l_{opt} on the template-dependent polymerization time per nt in a clay-water environment, t_{pol} , and on the time before present. The optimized polymer length is calculated as $l_{opt} = T_{st}/t_{pol}$. White and black dashed lines indicate l_{opt} of 10, 15, 20, 30 and 40 nts.

-
- [1] W. H. Yu, N. Li, D. S. Tong, C. H. Zhou, C. X. C. Lin, and C. Y. Xu, *Applied Clay Science* **80**, 443 (2013).
 - [2] U. Pedreira-Segade, J. Hao, A. Razafitianamaharavo, M. Pelletier, V. Marry, S. Le Crom, L. J. Michot, and I. Daniel, *Life* **8**, 59 (2018).
 - [3] L. H. de Oliveira, P. Trigueiro, B. Rigaud, E. C. da Silva-Filho, J. A. Osajima, M. G. Fonseca, J.-F. Lambert, T. Georgelin, and M. Jaber, *Applied Clay Science* **214**, 106234 (2021).
 - [4] S. Q. Zhou, Y. Q. Niu, J. H. Liu, X. X. Chen, C. S. Li, W. P. Gates, and C. H. Zhou, *Clays and Clay Minerals* **70**, 209 (2022).
 - [5] M. Franchi, J. P. Ferris, and E. Gallori, *Origins of Life and Evolution of the Biosphere* **33**, 1 (2003).
 - [6] J. P. Ferris, *Philosophical Transactions of the Royal Society B: Biological Sciences* **361**, 1777 (2006).
 - [7] J. H. Rosenberger, T. Göppel, P. W. Kudella, D. Braun, U. Gerland, and B. Altaner, *Physical Review X* **11**, 031055 (2021).
 - [8] C. Fernando, G. Von Kiedrowski, and E. Szathmáry, *Journal of Molecular Evolution* **64**, 572 (2007).
 - [9] M. Farhat, P. Auclair-Desrotour, G. Boué, and J. Laskar, *Astronomy & Astrophysics* **665**, L1 (2022), URL <https://doi.org/10.1051/0004-6361/202243445>.